Review article

Recent advances in multi-layer composite polymeric membranes for CO_2 separation: A review

Zhongde Dai, Luca Ansaloni, Liyuan Deng*

Department of Chemical Engineering, Norwegian University of Science and Technology (NTNU), Trondheim, 7491, Norway

Abstract

The development of multilayer composite membranes for CO_2 separation has gained increasing attention due to the desire for energy efficient technologies. Multilayer composite membranes have many advantages, including the possibility to optimize membrane materials independently by layers according to their different functions and to reduce the overall transport resistance by using ultrathin selective layers, and less limitations on the material mechanical properties and processability. A comprehensive review is required to capture details of the progresses that have already been achieved in developing multilayer composite membranes with improved CO_2 separation performance in the past 15−20 years. In this review, various composite membrane preparation methods were compared, advances in composite membranes for CO_2/CH_4 separation, CO_2/N_2 and CO_2/H_2 separation were summarized with detailed data, and challenges facing for the CO_2 separation using composite membranes, such as aging, plasticization and long-term stability, were discussed. Finally the perspectives and future research directions for composite membranes were presented.
© 2016, Institute of Process Engineering, Chinese Academy of Sciences. Publishing services by Elsevier B.V. on behalf of KeAi Communications Co., Ltd. This is an open access article under the CC BY-NC-ND license (http://creativecommons.org/licenses/by-nc-nd/4.0/).

Keywords: Composite membrane; CO_2 separation; Membrane fabrication; Membrane aging; Long-term stability

1. Introduction

Carbon dioxide (CO_2) is a greenhouse gas found primarily as a main combustion product of fossil fuel. It is also a component in natural gas, biogas, and landfill gas [1]. CO_2 in flue gas, which is generally emitted into the atmosphere, is one of the main contributions to global warming and climate change, while the presence of CO_2 in natural gas or biogas reduces the calorific value, and makes the gas streams acidic and corrosive. Therefore, the interest in removing CO_2 from natural gas and biogas gas, and CO_2 capture from syngas and flue gas, have driven the development of CO_2 separation process technologies.

In the past few decades, a large number of methods for CO_2 capture from various gas mixtures have been investigated and developed, such as chemical and physical absorption [2−4], solid adsorption [5,6], membrane [7−11], chemical looping [12−14], cryogenic [15], and gas hydrates [16,17]. In these technologies listed above, membrane separation processes hold many advantages, including lower capital and processing costs, smaller unit size, simpler operation, simpler up- and down-scaling, better energy efficiency, and much lower environmental impact [18].

CO_2 separation by membrane technology has experienced substantial growth, breakthroughs, and advances during the past few decades. Many new membrane materials and membrane processes have been developed and verified for CO_2 separation applications in both academia and industry since the late 1970s [19,20]. Several classification schemes have been reported for the placement of membrane/membrane processes into a variety of classes (as shown in Fig. 1).

Tremendous progress in CO_2 separation membranes has been made, and reports on CO_2 separation membranes have

---

* Corresponding author.
  E-mail address: deng@nt.ntnu.no (L. Deng).

increased in the past 10 years. A large number of review papers on membranes can be found from the material point of view, such as polymeric membranes [21,22], mixed matrix membranes [23−26], micro-porous membranes [27−31], MOF membranes [32], carbon membranes [33], ZIF membranes [34], polymer blend membranes [35], facilitated transport membranes [35,36], PEG-containing membranes [37], polyimide membranes [38], and ionic liquid-based membranes [39,40]. Some researchers also reviewed membranes from an application point of view, such as biogas upgrading [41−45], natural gas sweetening [19,46−49], CO$_2$ capture [50−53], hydrogen production [54−56], bio-hydrogen purification [57], olefin/paraffin separation [58], and petrochemical industry application [59]. Generally, in the abovementioned literatures, most of the data were collected from a single gas test for self-standing membrane with a thickness of around 50−150 μm and the separation performances were compared with the well-known 'Robeson upper bound' [60]. However, these data normally have big variations when compared with the industrial value, mainly because of two reasons: First, pure gas measurements are poor predictions of the industrial scale membrane performances, especially for CO$_2$ relevant separation processes; second, the permeation properties of composite membranes with a thin selective layer (usually 0.1−1.0 μm thick) are very different from thick films, the arrangement of the polymer chains in thin polymeric films may differ from bulk polymers [6,18], resulting in different transport properties, and consequently different separation performances [20].

Up to now, although a large amount of academic literature can be found using thin film composite membranes with a thin selective layer for gas separation, only a handful reviews can be found [61,62], and they are mainly focused on inorganic materials [63]. It is worth providing a comprehensive literature summary on the recent advances in multi-layer composite membranes for CO$_2$ separation. In this regard, different multi-layer composite membrane preparation/fabrication technologies are introduced in this paper followed by discussions on advances in different CO$_2$ separation applications (e.g. CO$_2$/CH$_4$, CO$_2$/N$_2$ and CO$_2$/H$_2$). In addition, challenges in composite membranes in industrial applications such as aging, plasticization, and the influence of impurities are also discussed. Finally, some conclusions are summarized and future work direction perspectives are proposed.

2. Overview of the multi-layer composite membrane

The motivation of fabricating ultra-thin, defect-free composite membranes is to achieve a high gas flux and to ensure the membrane gas separation processes are economically viable. Compared with integral asymmetric membranes prepared by the Loeb-Sourirajan technique, the principal advantages of composite membranes include fewer limitations on the material mechanical properties and processability, and a much smaller quantity needed to deposit the selective layer of a composite membrane (0.1−2 g/m^2), thus some high performance but expensive materials can be used.

2.1. Important parameters in membrane separation

Gas permeability (P_i, also called the permeation coefficient) and idea selectivity (α_{ij}^*) are the two key parameters used to evaluate the intrinsic permeability property of membrane materials for gas separation membranes, which can be expressed as:

$$P_i = \frac{l \cdot J_i}{\Delta p \cdot A} \tag{1}$$

where l is the membrane thickness, J_i is the gas flux of component i, while Δp is the partial pressure gradient across
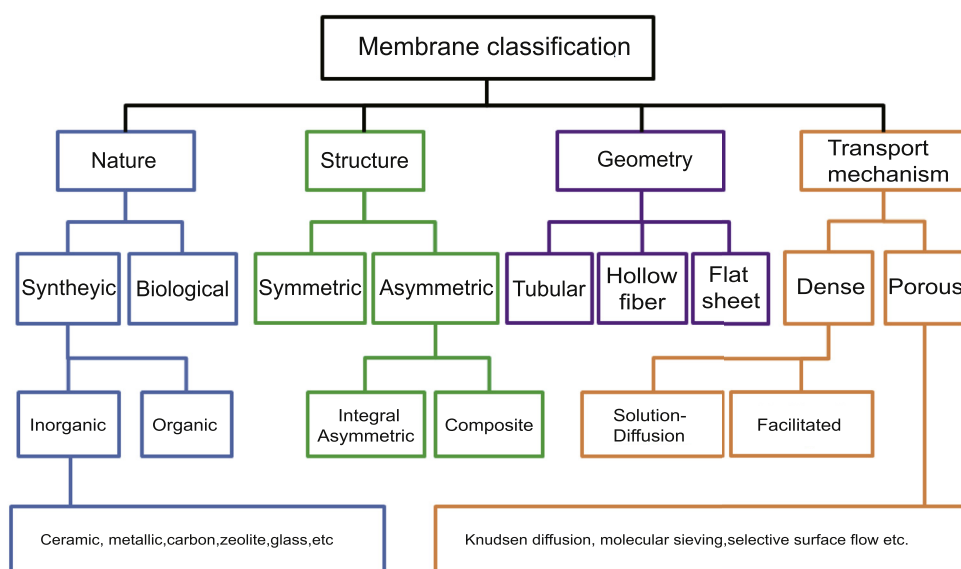

Fig. 1. Membrane classification.

Table 1
Conversion of different gas permeance units.

	(GPU) 10^{-6} cm^3(STP) cm^{-2} s^{-1} cmHg^{-1}	10^{-7} cm^3(STP) cm^{-2} s^{-1} kPa^{-1}	10^{-10} mol m^{-2} s^{-1} Pa^{-1}	10^{-3} m^3(STP) m^{-2} h^{-1} bar^{-1}
(GPU)10^{-6} cm^3(STP) cm^{-2} s^{-1} cmHg^{-1}	1	7.50	3.35	2.70
10^{-7} cm^3(STP) cm^{-2} s^{-1} kPa^{-1}	0.133	1	0.447	0.360
10^{-10} mol m^{-2} s^{-1} Pa^{-1}	0.299	2.24	1	0.806
10^{-3} m^3(STP) m^{-2} h^{-1} bar^{-1}	0.365	2.78	1.24	1

the membrane, and A is the effective membrane area. The most commonly used unit for permeability is Barrer, which is a non-SI unit named after Professor Richard Maling Barrer [64] (1 Barrer = 10^{-10} cm^3 (STP) cm^{-1} s^{-1} cmHg^{-1}).

Ideal selectivity (α_{ij}^*) is defined as the permeability ratio of two pure gases, as shown in Eq. (2).

$$\alpha_{ij}^* = \frac{P_i}{P_j} \tag{2}$$

where P_i and P_j are the permeability of gas species i and j in the membrane, respectively.

However, for composite membranes, permeance (Q_i) instead of permeability is commonly used to assess the membrane performances due to the unclear contribution of the layers to the mass transfer resistance and sometimes the thicknesses. Gas permeance can be expressed as:

$$Q_i = \frac{J_i}{\Delta p \cdot A} = \frac{P_i}{l} \tag{3}$$

Many different units has been used to present the permeation results. The most commonly used unit for gas permeance is GPU (gas permeation unit). However, other units are also widely used. For an easier comparison, the permeance data reported in this paper are all in GPU. The conversion rate between different units is given in Table 1.

The separation factor is commonly used instead of the ideal selectivity in reporting composite membranes that usually tested with mixed gases, where the real separation factor is not always equal to the idea selectivity due to the interaction and competition between the gases, and the concentration polarization effects in some highly permeable membranes. The separation factor is calculated from the ratio of the composition of the feed gas to the permeant gas, which can be expressed as:

$$\alpha_{ij} = \frac{y_i/x_i}{y_j/x_j} \tag{4}$$

where y_i and y_j are the molar fraction of gas species i and j on the permeate side, while x_i and x_j are the molar fraction of gas species i and j on the feed side. Unlike the permeability (P_i) and idea selectivity (α_{ij}^*), which are considered as material properties of a polymer, the permeance (Q_i) and separation factor (α_{ij}) are more sensitive to operation conditions (e.g. upstream and downstream pressure and feed gas composition). When the upstream partial pressure of a gas is much greater than that in the downstream, or the downstream partial

pressure is very low (e.g. a vacuum), the separation factor (α_{ij}) can be approaching the idea selectivity (α_{ij}^*) [21].

$$\alpha_{i,j} = \frac{y_i/y_j}{x_i/x_j} = \frac{1}{x_i/x_j} \frac{P_i}{P_j} \frac{p_{f,i} - p_{p,i}}{p_{f,j} - p_{p,j}} \approx \frac{P_i}{P_j} = \alpha_{ij}^* \tag{5}$$

2.2. Composite membrane structure

Fig. 2 presents a typical multi-layer composite membrane structure. Generally, a multi-layer composite membrane is fabricated by depositing different materials on a porous support. It generally contains at least a porous support and a selective layer, and for many cases, a gutter layer between the porous support and selective layer, and a protective layer above the selective layer.

In composite membranes, different layers contribute various functions to the composite membrane, thus their requirements on the properties are also different. The porous support mainly offers mechanical strength, therefore the support should have high porosity and low mass transfer resistance. In addition, the material should be cheap and easy to process into a porous structure. The main purpose of employing a gutter layer between the selective layer and porous support is to reduce the possible penetration of the coating solution into the membrane pores. It can also help to reduce the surface roughness of the support. The selective layer is the core part of a composite membrane, which offers the main separation properties of the membrane. Ideally, high gas permeance and high selectivity are the first two selection criteria for a selective layer membrane material, while other properties such as life-time, cost, aging, and stability, should also be considered. With the purpose of protecting the membrane during handling and fabrication into membrane modules, a protective layer can be employed if needed. More details about these different layers will be discussed in Sections 2.2.1−2.2.4.
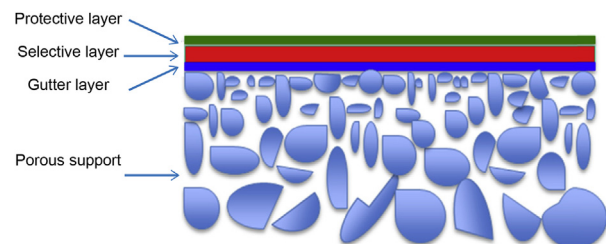

Fig. 2. Typical structure of a multi-layer composite membrane.

2.2.1. Porous support selection

The porous support in a composite membrane is normally made from the phase inversion method, which involves the precipitation of a casting solution by immersion in a non-solvent bath (NIPS). By far, the phase inversion process remains the primary method to prepare commercial gas separation membranes, such as polyimide (PI) and polysulfone (PSf). By controlling the membrane preparation conditions, the support can possess sponge-type structures or finger-like structures. For example, by choosing different solvents, controlling additive ratios, finger-like structures and sponge-type structures can be obtained for a PI membrane, as shown in Fig. 3(A) and (B) [65]. Generally, polymer consumption is roughly around 50 g/m^2 for asymmetric porous support prepared by phase inversion methods, in which the support and top dense layer are both made from the same material. Therefore, it is hard to commercialize the membranes of expensive polymers by this membrane preparation method if the phase inversion method works for them.

The stretching method is generally utilized to prepare porous membranes made of polymers that are not soluble in commonly used solvents. This technology normally consists of 4 steps: Heating, extruding, annealing, and stretching. The polymer is first heated to a melting state and followed by extruding the polymer as a nonporous polymer film. The annealing step is applied to improve the crystalline structure of the polymer film, thus facilitating the formation of a porous structure in the stretching step. The annealed film is then stretched to form micropores [66]. Porous polypropylene (PP) and polytetrafluoroethylene (PTFE) membranes are commonly prepared by this method. Fig. 3(C) and (D) shows the surface and cross section of a porous PP membrane prepared by using this method. It is clearly shown that the membrane prepared by using this method presents a symmetric structure.

So far, only a handful of commercially available polymer membranes have been reported as porous support. The commonly used porous supports are listed in Table 2.

Generally, an uncoated porous support should have a much higher gas flux (at least 10 times) than the coated one, which ensures most of (over 90%) the membrane resistance lies within the selective layer. In addition, the porous support should have a clean and smooth surface for an even and defect-free coating. In Table 2 it shows that some porous supports may have a very thin "dense" top surface layer without pores. In this case the support material can also contribute to the selectivity of the process depending on the intrinsic property of the material, while the porous structure under the surface can reduce the mass transfer resistance.
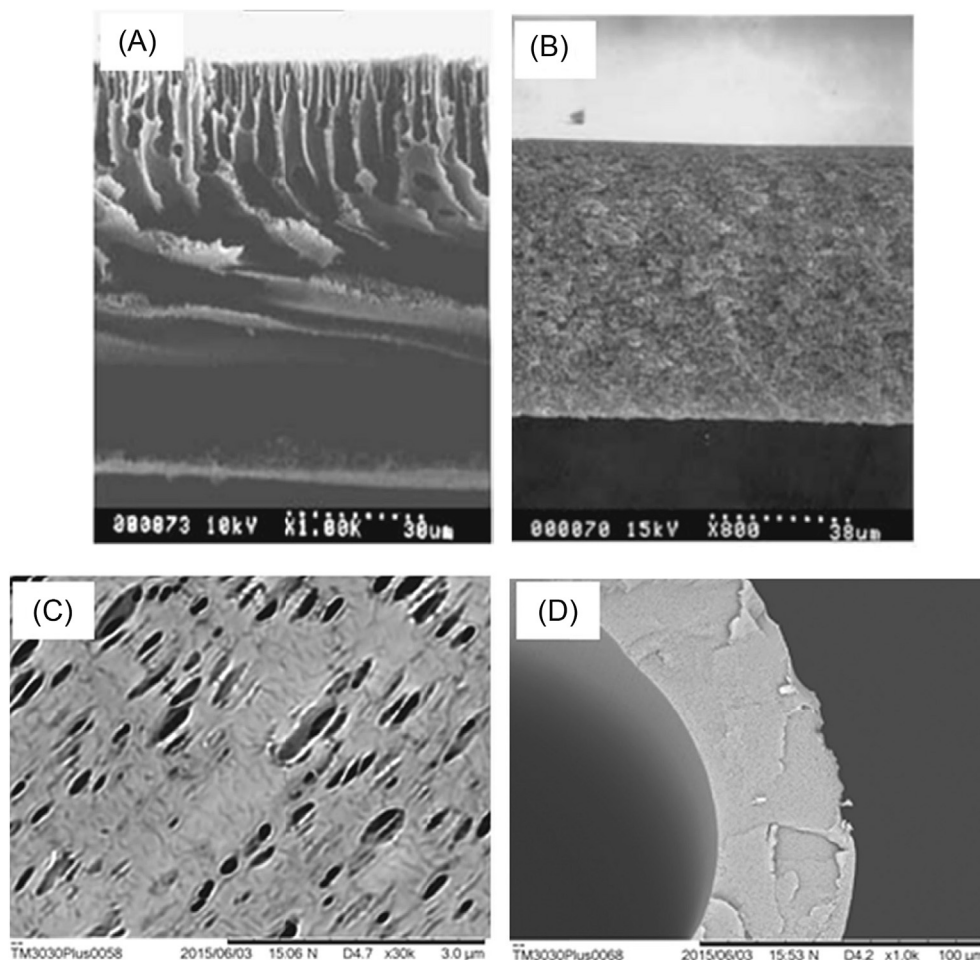

Fig. 3. Porous support prepared from phase inversion (A), (B) [65] and stretching (C), (D).

Table 2
Commonly used porous support in gas separation composite membranes.

Polymer	Preparation methods	Structure	Surface pore size range	Ref.
PSf	Phase inversion	Asymmetric	Dense to a few μms	[67−70]
PAN	Phase inversion	Asymmetric	Dense to a few μms	[71,72]
CA	Phase inversion	Asymmetric	Dense to a few μms	[73]
PEI	Phase inversion	Asymmetric	Dense to a few μms	[74,75]
PES	Phase inversion	Asymmetric	Dense to a few μms	[76,77]
PVDF	Phase inversion	Asymmetric/symmetric	Few nms to a few μms	[78,79]
PPO	Phase inversion	Asymmetric	Dense & porous	[80,81]
PP	Stretching	Symmetric	A few nms to a few μms	[82]
PTFE	Stretching	Symmetric	A few nms to a few μms	[83−85]
Teflon	Stretching	Symmetric	A few nms to a few μms	[86,87]

2.2.2. Gutter layer materials

A gutter layer can be applied between the selective layer and the porous support if needed. The gutter layer contributes differently in different cases. The main function of a gutter layer is to prevent the diluted polymer solution from penetrating into the porous structure and blocking the pores. In addition, a gutter layer should be sure of a smoother membrane surface, thus it is easier to coat a thin selective layer and make it 'defect-free'. Highly permeable polymers such as polydimethylsiloxane (PDMS) and poly(1-(trimethylsilyl)-1-propyne) (PTMSP) are the most commonly used (the chemical structures shown in Fig. 4) to fabricate the gutter layer.

However, although PTMSP is the polymer with the highest gas permeability (a permeability of CO_2 of around 19,000 to 37,000 Barrers) [88,89], the polymer will lose its performances within a very short time (as shown in Fig. 5). A reduction of 80% CO_2 permeance was observed for a PTMSP composited membrane coated on a polyacrylonitrile (PAN) support during an operation period of 14 days, while PDMS has a reduction of only around 5% during the same operation period. PDMS is a rubbery polymer with a reasonably stable performance over time. It has become the most commonly used gutter layer material up to now. It is worth mentioning that for PDMS membranes, cross-linking is also commonly used to improve the long-term stability. Cross-linking can also partly solve the physical aging problem in PTMSP [90,91].

2.2.3. Selective layer materials

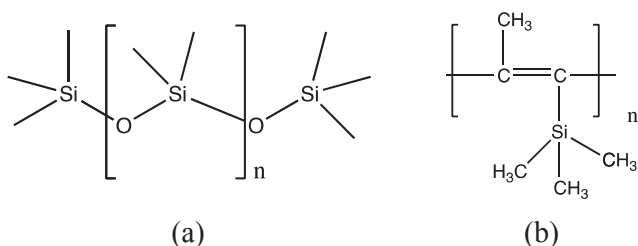In recent decades, hundreds, and even thousands of different polymers have been studied for gas separation in the
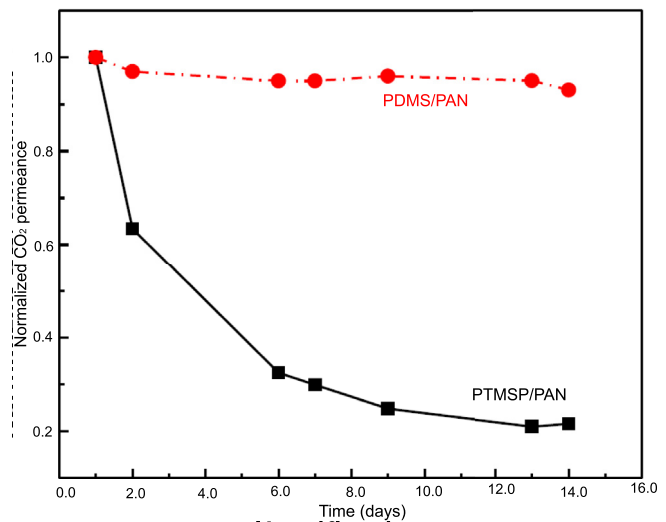

Fig. 5. Normalized CO_2 permeance of PDMS/PAN and PTMSP/PAN composite hollow fibers as a function of time, reproduced from Ref. [90].

form of thick dense membranes (with a thickness of around 50−150 μm), but only a handful of them have been applied to fabricate thin film composite membranes, and even fewer have found their commercial applications [20]. For example, glassy polymers with a rigid backbone and high free volume like PIM-1, PI show very promising gas separation performance in the thick dense membrane form. However, the accelerated physical aging in the thin film form results in losing their superior gas transport properties in a very short time [92]. Another example is the mixed matrix membrane, which consists of an inorganic filler incorporated into a polymeric matrix: A well-known route to enhance the properties of polymeric membranes. Although they show interesting results in the thick membrane form, the interfacial defects caused by the poor contact at the inorganic filler/polymer interface brings big challenges to maintain the gas selectivity when applying them in a thin film form.

The selective layer is the key part of the composite membrane, as it offers the separation function of the membrane. Ideally, materials to be used in the selective layer of a composite membrane for a successful CO_2 separation must meet the following criteria:

- High gas permeability is the primary requirement of a selective layer material, as a high gas flux can effectively reduce the membrane area needed and thus reduce the capital cost.
- High selectivity of CO_2 over other gases can effectively reduce the stage cut, consequently reducing the amount of gases needed for circulating, which is normally needed to meet the product purity requirement.
- Good thermal and chemical stability are also required to ensure a reasonable membrane life-time, as many gas treatment processes have relatively harsh conditions (e.g. high temperature/pressure), and very often there are impurities in the gas streams that may attack the membrane materials (e.g. SO_x and NO_x in flue gas).

Fig. 4. Chemical structure of PDMS (a) and PTMSP (b).

- Resistant to CO_2 plasticization is another requirement, especially for applications with high CO_2 partial pressures, which reduce the selectivity of the membranes.
- The membrane should also be resistant to aging, as physical aging tends to reduce the gas permeation performance of the membrane over time.
- The membrane material should be cost effective and able to be readily manufactured into different membrane modules. Low price and easy processability can effectively reduce the membrane module price and make the membrane more competitive to other separation technologies.

In the past few decades, many different polymers have been applied to fabricate multilayer composite membranes, such as polyimides, polyamides, block copolymers, and hydrophilic polymers with various amino groups. Basically, they can be divided into two categories according to the gas transport mechanisms: Solution-diffusion mechanism and facilitated transport mechanism. The mechanisms are illustrated in Fig. 6.

The most commonly studied transport mechanism in polymeric membranes is the solution-diffusion mechanism: Both the diffusivity and solubility of a gas contribute to the gas permeation. There is no chemical reaction involved in the gas transport. The driving force is the partial pressure of the gas between the feed side and the permeate side. This type of membrane is usually subjected to a trade-off between the gas permeability and selectivity [93].

A facilitated transport mechanism is another mechanism that involves reversible reactions between CO_2 and the functional groups in membranes. Compared to solution-diffusion membranes, facilitated transport membranes can have higher permeability and selectivity at a relatively low driving force. Another general characteristic of facilitated transport membranes is that the CO_2 permeability/permeance is pressure dependent, as the mobile carriers will be saturated under high CO_2 partial pressures and lose the facilitated transport properties, resulting in decreasing CO_2 permeability and consequently decreasing CO_2 selectivity over other gases, as shown in Fig. 7. More detailed discussion about facilitated transport membranes can be found in Refs. [94–96].

Since Ward et al. introduced facilitated transport membranes in 1967 [97], various facilitated transport membranes for CO_2 separation have been reported. In these membranes, amino groups (e.g. primary amine, secondary amine, and steric hindered amine) are the most commonly reported facilitated transport carriers. For example, polyvinyl amine (PVAm) is one of the most intensively studied polymeric membrane materials for CO_2 facilitated transport, in which the amino groups are defined as "fixed site carriers," as they can reversibly react with CO_2 and facilitate the CO_2 transport [94,98]. Water vapor is usually involved in this type of facilitated transport: CO_2 firstly reacts with water in the membrane promoted by the functional groups (facilitated transport carriers), and then transports quickly in the form of HCO_3^- ions, while the non-reactive gases like H_2, CH_4, and N_2 will transport through the membrane exclusively by the solution-diffusion mechanism; therefore the transport of CO_2 is greater than that of other gases, and consequently a high CO_2 selectivity can also be obtained. Compounds containing the carboxylate group (COO^-), the carbonate group (CO_3^{2-}), fluorion (F^-), potassium (K^+), and calcium (Ca^{2+}) have also been reported with facilitated transport effects [94,99,100]. It is worth mentioning that mimic enzymes containing a metal activation center have also been reported to facilitate the CO_2 transport in membranes [101,102]. As the advances in various categories of CO_2 separation membrane materials have been extensively reported in Refs. [21–31], a detailed description of the materials and their properties is not included in this paper.

2.2.4. Protective layer

A protective layer can be coated on the selective layer in a multi-layer composite membrane if needed. The protective layer has mainly two functions: To plug the small defects in the selective layer to improve the selectivity [103,104], and/or to protect the soft selective layer (e.g. Pebax) from being damaged in the membrane handling and membrane module fabrication process, especially in the fabrication of a membrane module with a high membrane packing density.

2.3. Fabrication of multi-layer composite membranes

The coating technique is essential in preparing a multi-layer composite membrane with a high performance. In the past few decades, various technologies have been developed to
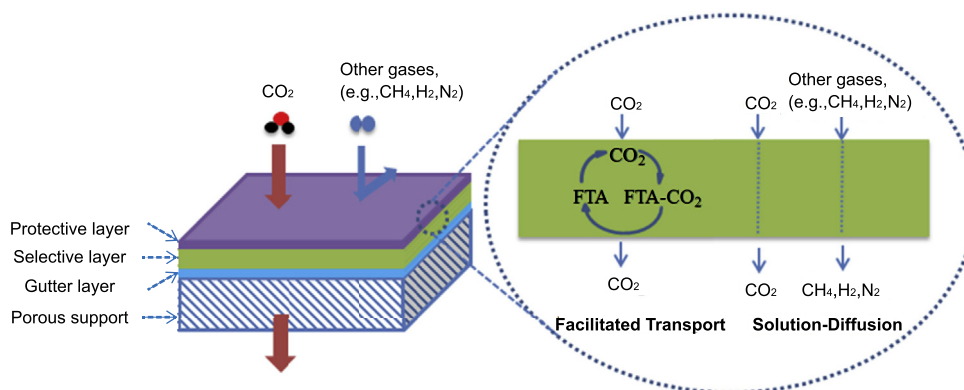

Fig. 6. Solution-diffusion and facilitated transport mechanism in a composite membrane. Reproduced from Ref. [40]. FTA represents facilitated transport agents.
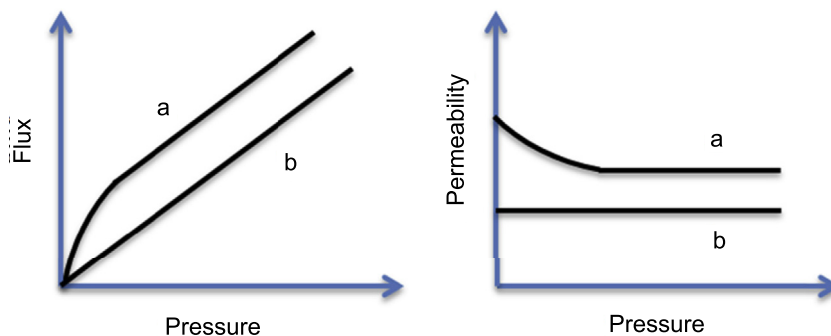
Fig. 7. CO_2 flux and permeability for membranes based on facilitated transport (a) and solution-diffusion transport (b). Reproduced from Ref. [94].

fabricate ultra-thin, defect-free layers. The most commonly used techniques are dip-coating, interfacial polymerization, and solution-casting.

2.3.1. Dip-coating

Currently, dip-coating is the simplest but most commonly used way to fabricate multi-layer composite membranes.

As shown in Fig. 8(A), in dip-coating, the composite membrane is prepared by coating the selective layer on the porous support by dipping the support into the polymer solution and lifting at a controlled speed. Normally a selective layer with a thickness of 0.05—2 microns can be prepared. The key parameters that need to be controlled in this process include the polymer solution concentration, the soaking time, the support withdrawal speed, as well as the evaporation environment (e.g. relative humidity, temperature). Fig. 8(B) is one example of composite membranes prepared by the dip-coating of a Pebax/PEG mixture solution on a porous PAN support.

Many mathematic models have been developed to predict the dip-coated layer thickness [106—108]. One of the commonly used models developed by Landau and Levich is shown in Eq. (6) [109]:

$$l = 0.944*Ca^{1/6}*\left(\frac{\eta U}{\rho g}\right)^{1/2} \tag{6}$$

where the Ca is a capillary number and defined as $Ca = \eta U/\sigma$, η is the viscosity of the liquid, U is the withdrawal speed, and σ is the surface tension of the liquid, ρ is the density of the liquid and g is the gravitational acceleration constant. It is worth noting that this method is only valid for low capillary number conditions; if the operation condition falls in the high capillary number regime, then another estimation model needs to be considered [110].

As a rule of thumb, gas flux through membranes is proportional to the selective layer thickness; therefore a thin and defect-free selective layer is normally preferred in order to achieve a high gas permeance. However, for facilitated transport membranes, the selective layer thickness cannot be optimized by simply reducing the coating layer thickness [111]. Schultz et al. suggested calculating the optimized facilitated transport membrane thickness based on the carrier complexation reaction rate and the Fickean diffusion rate using the second Damköhler number [112,113].

Compared to flat-sheet membranes, the hollow fibers are more commonly used in industry for gas separation, as they can offer a higher specific area per unit and a higher transmembrane pressure drop. Hollow fiber composite membranes can be coated from both the core side and shell side.

2.3.2. Interfacial polymerization

The preparation of composite membranes using interfacial polymerization was developed by John Cadotte, and North Star Research further developed this technology [114]. Composite membrane prepared by interfacial polymerization is
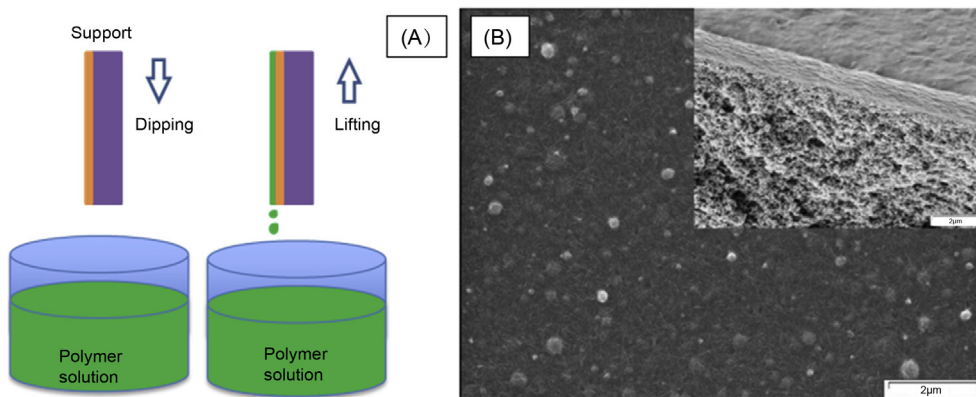

Fig. 8. Schematic of the dip-coating process (A) and an SEM image of a composite membranes prepared by the dip-coating method (B), reproduced from Ref. [105].

mostly used in water treatment. As the relatively thin selective layer (around 100 nms), the water flux can be high with a perfect salt rejection rate.

A composite membrane prepared by interfacial polymerization was considered unsuitable for gas separation, as in the interfacial polymerization process, a less cross-linked hydrogel is formed in the pores of the support. When this membrane is dried and applied for gas separation, the gel becomes a rigid network and adds large resistance to the gas transfer, thus resulting in very low gas fluxes [114].

In 1991, Baker et al. first introduced a gutter layer prior to the interfacial polymerization to prepare a membrane for gas separation [115]. Later on, Wang et al. used the same method to prepare interracially polymerized membranes for CO_2 separation [99] (as shown in Fig. 9). Small molecular amines with different structures were employed to react with the trimesoyl chloride (TMC) and resulted in a thin selective layer with a thickness of around 100 nms. The gutter layer can effectively prevent the penetration of the monomer solution into the pores, and thus solves the problem of hydrogel formation in the support pores. Parameters in the interfacial polymerization process include monomer concentration, polymerization time/temperature and curing conditions (e.g. curing time and temperature). Fig. 9 shows the schematic of the interfacial polymerization with a gutter layer (left) and the SEM image of a composite membrane prepared by interfacial polymerization of TMC and amines on a PSf porous support with a PDMS gutter layer on top.

2.3.3. Solution-casting

Solution-casting is the most straightforward method of fabricating a composite membrane. A coating applicator is normally used to cast the polymeric solution on a porous support. By carefully controlling the pre-set wet coating thickness (the gap between the substrate and coating knife) and the polymer concentration, the coating layer thickness can be effectively controlled. Generally, the thickness of the

selective layer prepared by this method can vary from below 1 μm to a few dozen μms. Fig. 10 shows the typical procedure of the multi-layer composite membrane preparation using the solution-casting method.

As the thickness of the selective layer is controlled by a coating applicator, it is challenging practically to prepare membranes with a selective layer lower than 1 μm.

2.3.4. Spin-coating

Spin-coating is widely used in the micro-fabrication of oxide layers using sol−gel precursors [117]. It has been also applied for preparing polymeric multi-layer composite membranes in the lab scale. In this process, the membrane is first fixed on a horizontal substrate, followed by dropping the proper amount of polymer solution onto the support (as shown in Fig. 11(A)). The substrate is then rotated or spun at a high speed. Centrifugal force causes the solution to spread into a thin film, while the solvent rapidly evaporates to yield a uniform solid polymer coating on the substrate. Fig. 11(B) shows an SEM image of a composite membrane prepared by using this method, in which the selective layer was obtained by spin-coating of polyimide polydimethylsiloxane triblock copolymer solution on a PAN substrates (40 mm) at a speed of 1000 rmp for 10 s. The thickness of the coating layer can be adjusted by controlling either the coating solution concentration or the spinning speed.

2.3.5. Chemical vapor deposition

The chemical vapor deposition (CVD) technique has been mainly used for the deposition of inorganic thin films. However, the CVD of polymeric thin films has become a new research topic in the past few years and has been applied in different fields [118]. For example, CVD has been used for polymeric membrane surface modification, membrane pore size control, and composite membrane deposition [119−121]. The separation performance of these composite membranes can be tuned by controlling the density and the thickness of the
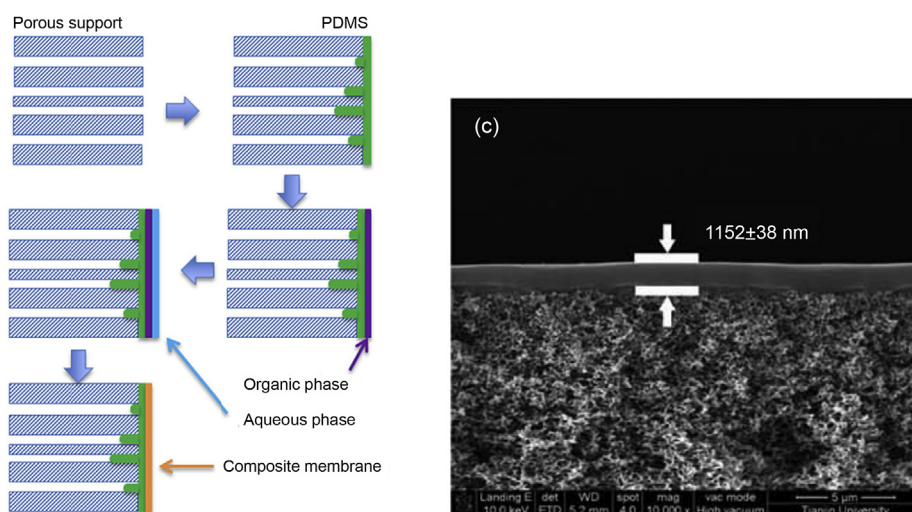

Fig. 9. Schematic representation of the preparation process of the membrane by interfacial polymerization with a gutter layer (left), and an SEM image of composite membranes prepared by the interfacial polymerization method (right), reproduced from Ref. [99].
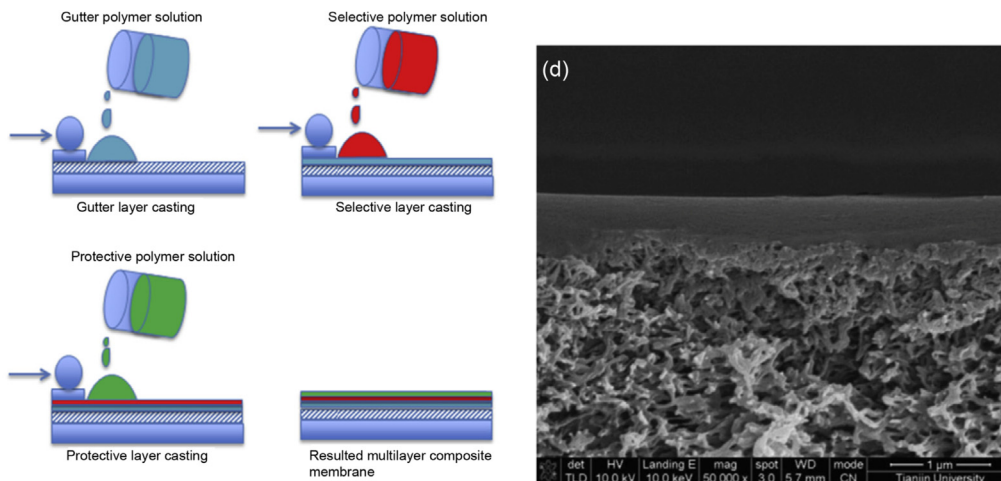
Fig. 10. Schematic representation of the solution-casting method (left) and an SEM image of composite membranes prepared by the solution casting method (right), reproduced from Ref. [116].
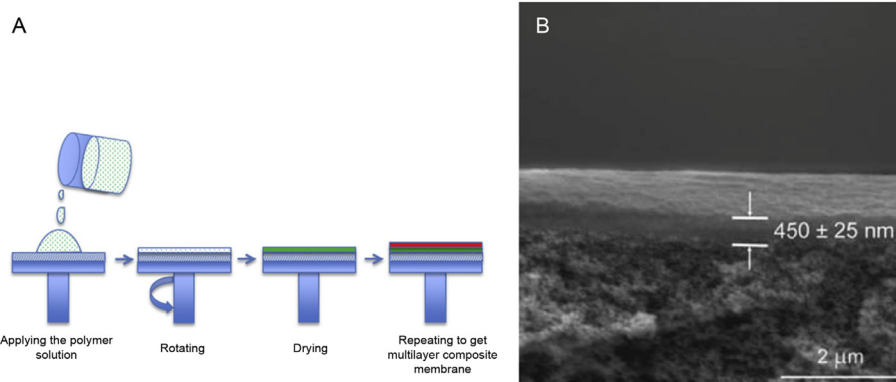

Fig. 11. Schematic of spin-coating process (A) and an SEM image of a composite membrane prepared by spin-coating method (B), reproduced from Ref. [71].

top layer. Compared with other methods used to fabricate multi-layer composite membranes, the gas phase in a CVD process can be directly converted to thin films. By eliminating the need to dissolve macromolecules, CVD holds the possibility of preparing multi-layer composite membranes from insoluble polymers and highly cross-linked organic networks.

2.3.6. Post-treatment

It is worth mentioning that besides the selective layer thickness, which is a key parameter that needs to be controlled during membrane fabrication, the post-treatment process also has considerable effects on the final membrane properties. It has been reported that even for the same material, different post-treatment could lead to huge differences in gas separation performances. Generally, different research groups tend to use different post-treatment strategies. For example, Cai et al. and Li et al. kept the membrane in a box with a constant relative humidity for a period of time before drying it [122,123]. Zhao et al. And Zou et al. tends to put the freshly coated membranes into a high-temperature oven for a few hours to further crosslink the PDMS gutter layer and remove the residual solvent in the membranes [124,125].

Apart from the methods mentioned above, there are more technologies for membrane coating, such as spray coating [126], brush coating [127], layer-by-layer deposition [128,129], as well as ultrasonic deposition [130,131]. However, they are not commonly used for gas separation applications, and hence are not discussed in this review.

3. CO$_2$ separation applications

3.1. CO$_2$/N$_2$ separation

Power generation from fossil fuel-fired power plants (e.g. coal and natural gas) is the single largest source of CO$_2$ emissions. The main composition of flue gas from different fossil fuel recourses is listed in Table 3. The majority of the flue gas is N$_2$ (78−80%) with a part of CO$_2$ (10−15%) and small amounts of different impurities such as NO$_x$ and SO$_x$.

Up to now, amine absorption seems the most mature technology, and it has been successfully used to treat CO$_2$-contained industrial gas streams for decades [2,132]. Membrane is considered an environmentally-friendly and energy-efficient alternative with great potential, but membranes with

both high CO_2 permeability and CO_2/N_2 selectivity must be utilized to be economically competitive with amine absorption for CO_2 capture from flue gas.

During the last decade, a large number of new membranes have been developed in lab scale, and several of them have been tested in a pilot scale. The reported membranes with detailed information on the membrane selective layer materials, porous supports, morphology, fabrication techniques, as well as the membrane separation performances are summarized, as listed in Table 4.

As can be seen, the composite membranes listed in Table 4 were prepared mainly by solution casting or dip-coating, and PVAm has been the most studied polymers [68,81,98,148−151]. Different strategies were used to improve the CO_2 transport properties, including copolymerization with other functional groups, incorporating with nano-sized particles, or blending with other compounds that can have strong interactions with CO_2. Wang et al. and Deng et al. studied incorporating different nano particles (e.g. MOF particles, PANI nanofibers, fumed silica nanoparticles, and CNT) into a PVAm polymeric matrix, and the gas separation properties of these mixed matrix membranes were investigated [152,173]. It is commonly accepted that the inorganic particles tend to aggregate and form bigger size particles in the membranes. However, they successfully fabricated composite membranes with around 1−10 μms without defects. By modifying the surface of the nanoparticles with some functional groups such as $-NH_2$, the adhesion between the particles and polymeric materials can be improved and result in higher gas selectivity [174]. Polymeric nanoparticles were also blended with Pebax to enhance the gas separation performances by Fu et al., and by optimizing the nanoparticle size/content in the nano-composite membrane, a CO_2 permeance of over 1500 GPU with a CO_2/N_2 selectivity of around 30 being fabricated [161].

Yave et al. systematically investigated different copolymers with polar ether segments, such as different grades of Pebax and polyactive [72,137], which are commercially available polymers with a relatively low price and holds the potential of further scaling up. The PDMS gutter layer was usually employed in their membranes, and low molecular weight CO_2-philic solvents, such as PEG, were used as additives to enhance the separation performances. By carefully optimizing polymer molecular weight, casting solution concentration, as well as the end groups of the free PEG-based additives, membranes with a selective layer of as low as around 50 nms

can be formed with extraordinary CO_2 separation performances [72,137].

Scofield et al. studied the incorporation of different PEG copolymers to a Pebax polymeric matrix to enhance the CO_2 transport. Both the gutter layer and the selective layer were fabricated by a spin-coating process. The resulted membrane showed similar CO_2/N_2 selectivity, but much higher CO_2 permeance than the pristine membrane without the additives [141]. Several researchers have also tried to incorporate various ionic liquids with polymers to prepare membranes with better CO_2 separation performance [40,175,176].

Ho and coworkers also studied facilitated transport membranes for post-combustion CO_2 capture, specifically at relatively high temperatures [177]. According to their results, high temperature can promote the reaction between CO_2 and the facilitated transport agents in the membrane, therefore high selectivity and high gas permeability can be obtained at the same time.

It is worth mentioning that Koschine et al. fabricated composite membranes with high free volume polymer (PIM-1), and by incorporating 2 wt% MWCNT into the polymer, the physical aging rate of the membrane was effectively reduced. CO_2 permeance show a reduction of 17% over a storage time of 300 days, while the corresponding pristine PIM-1 membrane without CNT showed a CO_2 permeance reduction of 38% [172]. This suggests that by properly selecting inorganic fillers, the physical aging problem of high free volume polymer can be partly solved and the membrane may be promising for further applications.

Most of the aforementioned membranes are flat sheet membranes. Chen et al. investigated the possibility of coating a layer of Pebax on a porous PAN hollow fiber support for CO_2/N_2 separation [90]. PDMS was used as the gutter layer in their study. Different parameters such as coating solution concentration and coating time on gas separation performance were investigated and optimized [90]. They also investigated the influence of adding ILs into the Pebax matrix. It was found that the free ILs can enhance both the solubility and diffusivity of the gas, thus enhanced CO_2 permeability and selectivity of CO_2 over other gases can be obtained. However, it was challenging to fabricate a defect-free composite membrane with a Pebax-IL mixture.

The possibility of post-combustion CO_2 capture using an amino group-based fixed-site carrier (FSC) membrane has been intensively investigated by Hägg and coworkers in the lab scale and pilot scale with both flat sheet and hollow fiber membranes. Different parameters in the membrane preparation process were systematically investigated, such as coating solution concentration, casting solution pH, membrane thickness, relative humidity, as well as membrane swell ratio [98,151,178]. Attempts were also made by blending the PVAm with different compounds (e.g. PVA and nanoparticles) to improve the properties of the membrane. Membranes with a CO_2/N_2 selectivity of over 200 have been developed with a reasonable lifetime. A pilot-scale membrane module with a membrane surface of over 10 m^2 has been applied in the cement industry for a pilot-scale test over a period of 9 months [179]. According to the results, the membrane showed good stability under real industrial operation conditions.

Table 3
Compositions of different flue gases from various fuels.

Chemical species	NG	Fuel oil	Coal
N_2	78−80%	78−80%	78−80%
CO_2	10−12%	12−14%	~10.6%
O_2	2−3%	2−6%	7%
CO	70−110 ppm	−	5579 ppm
NO_2	−	−	1%
NO	−	−	1%
SO_2	−	−	>2000 ppm
Ash	0	0	12%

Table 4
Composite polymeric membranes for CO_2/N_2 separation.

Selective layer material and thickness (μm)	Support layer materials/surface pore size (nm)[b]	Gutter layer material/thickness (μm)	Fabrication method	Feed gas	Operation conditions	CO_2 permeance (GPU)	CO_2/N_2 selectivity	Ref.
Pebax® 1657+ Pluronic F127 (0.1–0.8)	PES (4–11)	–	Casting	CO_2/N_2 (10/90 by volume)	3 bar, RT, 100% RH	1275–2420	46–100	[133]
Polaris (–)	–	–	–	–	–	1000	50	[134]
Polaris 2 (–)	–	–	–	–	–	2000		[135]
Pebax® 1657/PEG (<2)	PAN	Pebax® 1657	Dip-coating	CO_2/N_2 (25/75 by volume)	20 °C, 8 bar, dry state	93	70	[136]
Polyactive (~0.1)	PAN (~20)	PDMS	Dip-coating	Pure gas	60 °C, 1 bar, dry conditions	2330	30	[72]
				Pure gas	60 °C, 1 bar, humid conditions	5000	30	[72]
				CO_2/N_2 (15/85 by volume)	20 °C, 5 bar, dry conditions	~925	55	[72]
Polyactive+PEGBE (~0.15)	PAN (–)	PDMS	Dip-coating	CO_2/N_2 (28/72 by volume)	20 °C, 10 bar, dry conditions	~703	40	[137]
PBT-PEO (~0.05)	PAN (–)	PDMS	Dip-coating	Pure gas	–	1813	>50	[138]
PIL-IL (0.096)	–	3 M proprietary material	Two-step coating	Pure gas	Feed pressure 10 psi, dry conditions	6100	22	[139]
Pebax® 2533/HMA-PEO (0.18–0.6)	PAN (–)	PDMS (~0.18)	Spin-coating	Single gas	35 °C and 340 kPa, dry conditions	305–1190	14–24	[140]
Pebax+ fluorinated additives (0.35–0.91)	PAN (–)	PDMS (~0.35)	Spin-coating	Single gas	35 °C and 350 kPa, dry conditions	1160–1830	~22	[141]
Pebax-RTIL (0.3–1)	PAN (~15.7)	PDMS (~1) PTMSP	Dip-coating	CO_2/N_2 (50/50 by volume)	(HF)	350	37.6	[90]
PAMAM (~0.1)	PSf (–)	Chitosan (~0.2)	In-situ modification	CO_2/N_2 (5/95 by volume)	CO_2 partial pressure 97 kPa at 40 °C	61	230	[142]
P (DADMACA-co-VAm) (~0.5)	PSf (MWCO 6k)	–	Casting	CO_2/N_2 (15/85 by volume)	0.11 MPa, 100% RH	1850	160	[116]
PANI-PVAm (~3)	PSf (MWCO 6k)	–	Casting	CO_2/N_2 (20/80 by volume)	0.11 MPa, 100% RH	1200	120	[143]
DGBAmE and DAmPEG+TMC (0.8–1.22)	PSf (MWCO 6k)	PDMS (~0.8)	IP	CO_2/N_2 (15/85 by volume)	0.11 MPa, 100% RH	2200	62	[144]
DGBAmE+TMC (~0.15)	PSf (MWCO 6k)	PDMS (~0.8)	IP	CO_2/N_2 (15/85 by volume)	0.11 MPa, 100% RH	1601	138	[145]
DamBS and DGBAmE + TMC (<0.5)	PSf (MWCO 6k)	PDMS	IP	CO_2/N_2 (15/85 by volume)	0.11 MPa, 100% RH	200–400	60–120	[99]
MEDA-TMC (~0.14)	PSf (MWCO 6k)	PDMS	IP	CO_2/N_2 (15/85 by volume)	0.11 MPa, 100% RH	1035	87.0	[146]
DNMDAM-TMC (0.1–0.9)	PSf (MWCO 6k)	–	IP	CO_2/N_2 (15/85 by volume)	0.11 MPa, 100% RH	173	69.2	[147]

PVAM-eda (0.15−0.6)	PSf (MWCO 6k)	−	Casting	CO_2/N_2 (20/80 by volume)	25 °C, 1.1 bar, 100%RH	607	106	[68]
PVAm−PIP (0.13−0.78)	PSf (MWCO 6k)	−	Casting	CO_2/N_2 (20/80 by volume)	25 °C, 1.1 bar, 100%RH	6500	277	[148]
PVAm-PVA (~0.3)	PSf (MWCO 50k)	−	Casting	CO_2/N_2 (10/90 by volume)	25 °C, 2 bar, 100%RH	212	174	[98]
PVAm (0.7−1.5)	PPO (HF)[a] PSf (HF)	−	Coating	CO_2/N_2 (10/90 by volume)	25 °C, 5 bar, 100%RH	365	59.8	[81]
PEIE−HT and PEIE (~0.25)	PSf (MWCO 6k)	−	Casting	CO_2/N_2 (15/85 by volume)	0.11 MPa, 100% RH	5693	269	[149]
PVAm-ZiF-8 (0.140−0.387)	PSf (MWCO 6k)	−	Casting	CO_2/N_2 (15/85 by volume)	0.11 MPa, 100% RH	1500	105	[150]
PVAm/PVA (~0.3)	PSf (MWCO 50k)	−	Casting	CO_2/N_2 (10/90 by volume)	25 °C, 2 bar, 100%RH	307.1	162	[151]
PDMS-PDA-PVAm (0.5−1)	PSf (MWCO 6k)	PDMS	Casting	CO_2/N_2 (15/85 by volume)	25 °C, 0.11 Mpa, 100%RH	1887	83.1	[123]
Pebax 1657/PDA−PDMS (0.5−1)	PSf (MWCO 6k)	−	Casting	CO_2/N_2 (15/85 by volume)	25 °C, 0.11 Mpa, 100%RH	670	62	[123]
PVAm-inorganic particles (0.28)	PSf (MWCO 6k)	−	Casting	CO_2/N_2 (15/85 by volume)	25 °C, 0.11 Mpa, 100%RH	70−120	15.7−28.6	[152]
Poly(N-vinylimidazole)−zinc complex (~0.120)	PSf (MWCO 6k)	−	Casting	CO_2/N_2 (15/85 by volume)	25 °C, 0.11 Mpa, 100%RH	1150	95.8	[102]
PVA-mimic enzyme (0.76−0.85)	PSf (MWCO 50k)	−	Dip-coating	CO_2/N_2 (10/90 by volume)	RT, 1.7 Bar, 100% RH	255	107	[101]
PVP/KF electrolyte (−)	PSf	−	Coating	Single gas	1.5 kg f cm^{-2}	28	4.1	[153]
PVP+K salt (−)	PSf (~70)	−	Coating	Single gas	1.5 kg f cm^{-2}	52.01	25.6	[154]
PDMAEMA−PEGMEA (2.5)	PSf (HF, −)	−	Coating	Single gas	25 °C, 1 bar, humid conditions (HF)	25	31	[67]
PEGBEM-g-POEM (1.5−2.3)	PSf (~500)	−	Coating	Single gas	RT	1.3−117	2.1−84.7	[155]
Polyamines+PVA (~3)	PSf (~50)	−	Casting	$CO_2/H_2/N_2$ (20/40/40 by volume)	110 °C and a feed pressure of 2 atm	119−309 Barrer	179−366	[156]
PVA-fixed amine carriers (~30)	PTFE (200)	−	Casting	$CO_2/H_2/N_2$ (20/40/40 by volume)	110 °C and a feed pressure of 2 atm	6196 Barrers	492	[84]
PVAm-PANI (~0.52)	PSf (MWCO 6k)	−	Casting	CO_2/N_2 (15/85 by volume)	25 °C, 0.11 Mpa, 100%RH	3100	245	[70]
Amine-containing polymer/zeolite Y (~0.2)	PES (~72)	−	Dip-coating + casting	CO_2/N_2 (20/80 by volume)	57 °C, 1.7 PSIG	1100	>200	[157]
PEO-PBT/GO	PAN (−)	−	Dip-coating	−	−	24.9−80.3	41−72	[158]
Crosslinked-PVA−PVP (40−70)	PSf (~30)	−	Casting	CO_2/N_2 (20/80 by volume)	2.8 atm, 100 °C	29	270	[159]
Pebax-soft polymer nanoparticles (~0.58)	PAN (−)	PDMS (0.17)	Spin-coating	Single gas	35 °C, 3.4 bar	326−1374	24−12	[160]
Pebax-soft polymer nanoparticles (<0.3)	PAN (MWCO 6k)	PDMS (<0.2)	Spin-coating	Single gas	35 °C	414−1200	23−34	[161]
Pebax-soft polymer nanoparticles (~0.3)	PAN	PDMS (~0.255)	Spin-coating	Single gas	35 °C	468−1670	10−24	[162]
Cross linked PEG (<0.1)	PAN (−)	PDMS (~0.19)	Spin-coating	CO_2/N_2 (30/70 by volume)	35 °C	~1200	~22	[163]
PEG-PDMS BCP+Pebax (<0.1)	PAN	PDMS (~0.175)	Spin-coating	Single gas	35 °C and 350 kPa	~1000	21	[164]
Poly(fluoropropylmethylsiloxane) (PTFPMS) (10−50)	PEI (HF)	−	Dip-coating	Single gas	0.1−0.5 MPa	40−75	16.03−18.80	[165]
PTFPMS/PEG (~15)	PEI	−	Dip-coating	Single gas	0.1−0.5 MPa	56.3	26.7	[166]

(continued on next page)

Table 4 (continued)

Selective layer material and thickness (µm)	Support layer materials/surface pore size (nm)[b]	Gutter layer material/thickness (µm)	Fabrication method	Feed gas	Operation conditions	CO_2 permeance (GPU)	CO_2/N_2 selectivity	Ref.
PDMS (~0.2)	PAN (HF, 14.5–15.7)	PDMS (—)	Dip-coating	CO_2/N_2 (15/85 by volume)	25 °C and 2 atm	3700	10	[167]
Pebax (<1)	PVDF/PES (HF)	PTMSP/PDMS	Coating	CO_2/N_2 (22.54/77.46 by volume)	RT	550	45	[168]
Pebax (<5)	PSf		Dip-coating	—	25 °C and 100 psig,	61	~32	[169]
PDMS/MOF (<2)	PSf (HF)	—	Dip-coating	Single gas	25 °C at 5 bar	~110	~35	[170]
PVP/H₃BTC (~6.5)	PSf	—	Dip-coating	Single gas	RT, 2 atm	~1.2	8.5	[171]
PIM-1/CNT (~0.65–0.77)	PAN (~25)	—	Dip-coating	—	—	10,548	34.4	[172]
				—	—	8796(a)	37.1	[172]

[a] HF denotes hollow fiber membranes.
[b] The support membrane pore size either expressed as nm or molecular weight cut off (MWCO).

Enzymatic membranes are a special type of CO_2 facilitated transport membranes highlighted in recent years. Yao et al. developed membranes based on biomimetic material containing the zinc–poly(N-vinylimidazole) (PVI) complex to facilitate the hydration of CO_2 [102]. Membranes with a selective layer of around 120 nms were successfully fabricated with Zn(II) as the active site to simulate the enzyme function for CO_2 facilitated transport. Very recently, facilitated transport membranes containing a low molecular weight mimic enzyme (Zn-cyclen) were developed by Saeed and Deng using polyvinyl alcohol (PVA) as the polymer matrix [101]. With the presence of the mimic enzyme, both the CO_2 permeance and CO_2/N_2 selectivity were greatly enhanced. The permeance of CO_2 in a mimic enzyme PVA membrane is 5 times greater as compared to that in a PVA membrane with a doubled CO_2/N_2 selectivity.

In 2013, Oh et al. reported a poly(vinylpyrrolidone) (PVP)/Potassium fluoride (KF) electrolyte membrane for facilitated CO_2 transport [153]. According to their results, the KF can reversibly interact with CO_2 molecules, and the resulted PVP/KF electrolyte membrane show enhanced CO_2 separation performance compared with a neat PVP membrane. In 2014, the same group introduced fluorosilicate anions $(SiF_5(H_2O)^-)$ to the same system, and it shows that the anion has a significant effect on the K^+ carrier activity, resulting in increased CO_2 transport compared to the previous F^- based membranes [154]. Even though these two polymer electrolyte membranes show relatively low separation performances, by properly choosing both the polymer matrix (e.g. Pebax) and the facilitated transport salt (e.g. Calcium phosphotungstate), different membranes with attractive results showing a CO_2 permeability of over 3500 Barrers with CO_2/N_2 selectivity over 70 was reported [180,181]. Furthermore, these membranes exhibited almost no apparent changes in permeability or selectivity during a 400-h continuous long-term stability test.

The main drawback for a facilitated transport membrane is that the CO_2 permeability (permeance) is dependent on CO_2 partial pressure, and at a high CO_2 partial pressure, the facilitated agents will be saturated by CO_2 and lose the facilitated transport effect. Nevertheless, for the post-combustion CO_2 capture, the total feed gas pressure is around 1 atm, with a CO_2 concentration of around 3%–15%; facilitated transport agents will not be saturated at such low CO_2 partial pressures, making facilitated transport membranes excellent candidates for post-combustion CO_2 capture.

3.2. CO_2/CH_4 separation

Natural gas (NG) consumption worldwide was 3393.0 billion cubic meters in 2014 [164], and this is growing every year, making natural gas processing the largest industrial gas separation application. Generally, most of the raw NG needs to be treated to meet pipeline specifications, as raw NG having a widely variable composition, including CH_4 (the main component of natural gas), water vapor, CO_2, H_2S, N_2, as well as heavier gaseous hydrocarbons, as listed in Table 5. The composition of these components varies depending on reservoir sources [48]. The availability of a simple process

Table 5
Typical natural gas compositions, adopted from Ref. [46].

Compounds	Concentration (mol%)
CH_4	29.98–90.12
C_2H_6	0.55–14.22
C_3H_8	0.23–12.54
C_4H_{10}	0.14–8.12
C_5H_{12} and heavier VOCs	0.037–3.0
CO_2	0.06–42.66
He	0.0–1.8
N_2	0.21–26.10
H_2S	0.0–3.3

technology that can be applied in remote, unattended, or offshore situations is highly desirable for NG processing and purification.

The two major processes in raw NG processing are gas dehydration and gas sweetening. CO_2 removal is the main part of NG sweetening, as CO_2 is the main acidic gas impurity in NG, as shown in Table 5. The necessity for CO_2 removal is not only to increase the fuel heating value, but also to reduce pipeline corrosion as well as preventing atmospheric pollution [182].

Membranes for NG processing were first commercialized in the 1980s for CO_2 removal [183], which has been the dominant membrane gas separation application since then. Commercial NG separation membrane materials include polyimides, cellulose acetate, as well as some perfluoro polymers and polysulfone (PSf). These membranes usually show a CO_2 permeance of around 100 GPU or less, with a CO_2/CH_4 selectivity of around 20 or less under real industry operation conditions [19].

In the past ten years, a large number of membrane materials (both inorganic and polymeric) have been synthesized and tested in the lab scale for CO_2 separation from CH_4, including different polyimides [38,184,185], polymers of intrinsic microporosity (PIMs) [186], thermal re-arranged (TR) polymers [28]. A large number of different organic/inorganic particles have also been introduced to fabricate mixed matrix membranes (MMMs) for NG sweetening [187–189]. Generally, these membrane materials were fabricated into membranes with a thickness of around a few μm to hundreds of μms. There have been many reviews summarizing these developments [19,48,190]. However, despite these great achievements in material development, many of these materials have limitations and are hard to fabricate into composite membranes (e.g. TR polymers, MMMs). Fortunately, there are also many polymers being fabricated into multilayer composite membranes with a selective layer around or lower than 1 μm: detailed information is given in Table 6. Some of them show much better separation performances (one magnitude higher CO_2 permeance) compared to the most commonly used cellulose acetate (CA) membranes under lab conditions.

As can be seen from Table 6, despite the different polymeric materials used, the main membrane fabrication technologies are dip-coating, solution casting, and interfacial polymerization (IP). With a thin selective layer, these membranes normally show much higher CO_2 permeance compared

to commercial CA membranes. For example, in Table 6 most of the up-to-date CO_2 separation data are better than the commercial CA membranes, and some of them exhibit much higher permeance and CO_2/CH_4 selectivity [116,145,194]. However, almost all the data were collected under controlled laboratory conditions using a synthetic binary or ternary gas mixture without impurities. Furthermore, separation tests were normally carried out at relatively low CO_2 partial pressure conditions. The performance of these membranes could have been overestimated for real conditions at much higher CO_2 partial pressure and the presence of impurities.

Generally, for a membrane based on facilitated transport, a decline in both CO_2 permeance and CO_2/CH_4 selectivity with increasing the CO_2 partial pressure can be observed. This is recognized as characteristic behavior of a facilitated transport membrane due to 'carrier saturation' [205]. As CH_4 is not involved in the facilitated transport, the feed pressure has a limited effect on CH_4 permeability (if the membrane is not plasticized by the high pressure CO_2), resulting in a decrease in the overall CO_2/CH_4 selectivity. For example, Li et al. developed a membrane with a CO_2 permeance of around 1600 GPU and a CO_2/CH_4 selectivity of about 85 at an operational pressure of 1.1 bar. By increasing the operation pressure to 30 bar the CO_2 permeance sharply reduced to around 200 GPU with a CO_2/CH_4 selectivity of lower than 30 [116]. Different facilitated transport membranes developed in the same group show similar phenomena [145]. Another factor that contributes to the reduction of CO_2/CH_4 selectivity is the membrane plasticization induced by the high CO_2 partial pressure, which tends to increase the permeability of all gaseous species.

The application of facilitated transport membranes containing PVAm in NG gas treatment at high pressures were also studied by Deng and Hägg at the lab scale and small size pilot [122,151,197]. The PVAm-based FSC membranes were optimized for high pressures. The CO_2 partial pressure shows considerable negative influence on both CO_2 permeance and CO_2/CH_4 selectivity in these membranes. The membrane structure and fabrication procedure were systematically investigated to develop more pressure-resistant membranes. The fabrication parameters, including blending with PVA, the post-treatment conditions and the addition of CNTs, were optimized and membranes with significantly improved performance reported [111,173]. The influences of impurities on the separation performances of the same membranes were intensively studied by Uddin et al. [196,206,207].

One concern for a facilitated transport membrane is that some of the impurities, such as H_2S and SO_2, may have a competitive reaction with the facilitated transport carriers in the polymeric matrix, which may reduce the CO_2 permeance as well as the selectivity of CO_2 over CH_4. The plasticization is another concern, especially for high CO_2 pressure applications. These will be discussed in more detail in Sections 4.2 and 4.3. With these concerns, people argue that the loss of separation performance between lab measurements and actual practice is greater than that occurs for CA or other PI membranes with CO_2 separation performances in the "low

Table 6
Composite polymeric membranes for CO_2/CH_4 separation.

Selective layer material and thickness (μm)	Support materials/surface pore size (nm)	Gutter layer/ thickness (μm)	Fabrication method	Feed gas	Operation condition	CO_2 permeance (GPU)	CO_2/CH_4 selectivity	Ref.
P (DADMACA-co-VAm) (~0.5)	PSf (MWCO 6k)	−	Casting	CO_2/CH_4 (15/85 by volume)	0.11 MPa, 100%RH	1636	86.5	[116]
DGBAmE and DAmPEG+TMC (0.8−1.22)	PSf (MWCO 6k)	PDMS (~0.8)	IP	CO_2/CH_4 (15/85 by volume)	0.11 MPa, 100%RH	2200	86.9	[144]
DGBAmE+TMC (−)	PSf (MWCO 6k)	PDMS (~0.8)	IP	CO_2/CH_4 (15/85 by volume)	0.11 MPa, 100%RH	1601	31.4	[145]
Functionalized PANI (~130)	PP (43)	−	In situ deposition	CO_2/CH_4 (10/90 by volume)	128 kPa feed, RT	3470 Barrers	490	[191]
Polaris (0.05−0.2)	−	−(0.05−0.2)	Dip-coating	Pure gas	0.1 MPa, −10 °C	150	39	[192]
DEA-crosslinked PVA (−)	PTFE (100)	−	Casting	CO_2/CH_4 mixture	Humid conditions, RT	0.621−18.1	7.76−136	[83]
DNMDAM-TMC (0.1−0.3)	PSf (MWCO 6k)	−	IP	CO_2/CH_4 (10/90 by volume)	0.11 MPa, humid conditions, RT	118	37	[147]
PETEDA-PVA (~4)	PES	−	Casting	CO_2/CH_4 (10/90 by volume)	143.5 cmHg, humid conditions, RT	69,4	19	[193]
Hydrolysized PVP (−)	PSf (MWCO 50k), PES (MWCO 30k), PAN (MWCO 50k)	−	Casting	CO_2/CH_4 (50/50 by volume)	RT, humid conditions	390	50	[194]
PVAm-PEG (−)	PES (−)	−	Casting	−	96 cm Hg of feed pressure	5,8	63.1	[195]
PVAm/PVA (~0.65)	PSf (MWCO 50k)	−	Casting	CO_2/CH_4 (10/90 by volume)	RT, 2 bar, 80%RH	35,6	32	[196]
PVAm-PVA-CNT (~0.7)	PSf	−	Casting	CO_2/CH_4 (10/90 by volume)	2−5 bar, RT	129.5	45	[173]
PVAm/PVA (0.3−0.7)	PSf (MWCO 50k)	−	Casting	CO_2/CH_4 (10/90 by volume)	2−5 bar, RT	203.5	45	[151]
PVAm/PVA (~0.5)	PSf (−)	−	Casting	CO_2/CH_4 (35/65 by volume)	2−5 bar, RT	203.5	5.0	[197]
PAAm-PVA (~3)	PSf (MWCO 30k)	−	Casting	CO_2/CH_4 (10/90 by volume)	0.11 MPa, humid conditions, RT	112.5	15	[122]
PVAm (~20)	PES (MWCO 10k), PSf (MWCO 30k), CA (MWCO 20k), PAN (MWCO 75k)	−	Coating	Mixed gas	25−35 °C, 2~4 bar, humid conditions	5.18	>1000	[198]
PVAm-CNT (2−3)	PSf (MWCO 20k and 50k)	−	Casting	CO_2/CH_4 (10/90 by volume)	Humid conditions, 2 bar	81	23	[199]
PVAm-CNT (2−3)	PSf (MWCO 20k)	−	Casting	CO_2/CH_4 (10/90 by volume)	Humid conditions, feed pressure up to 40 bar	30.6−79.6	17.9−34.7	[200]
Poly (4-vinylpyridine)/Silicone rubber (~1)	PSf (HF)	−	Dip-coating	Pure gas	200 psi, RT	92	29	[201]
PVA-PVAm (0.6−2)	PSf (MWCO 20k and 50k)	−	Solution casting/ dip-coating	CO_2/CH_4 (10/90 by volume)	Humid conditions, 2~5 bar	214.6	46	[111]
PVA-CNT-amine (10−30)	PSf (10) PTFE (>30)	−	Casting	20% CO_2, 20.2% H_2, 59.8% CH_4	2−28 bar and 103 −121 °C	957 Barrers	3.63	[202]
PEO-PBT/GO (−)	PAN (−)	−	Dip-coating	Pure gas	RT	24.9−80.3	18−21	[158]
PVAm-inorganic particles (0.28)	PSf (MWCO 6k)	−	Casting	CO_2/CH_4 (15/85 by volume)	25 °C, 0.11 Mpa, 100% RH	70−120	8.91−10.9	[152]
PDMS/MOF (<2)	PSf (HF)	−	Dip-coating	Single gas	25 °C at 5 bar	~110	~32	[170]
TETA/TMC (~0.2)	PES (MWCO 30k)	−	IP	CO_2/CH_4 (10/90 by volume)	RT, 1.1 atm	13.3	94.1	[203]
Pebax (~5)	PAN (HF, 10−100)	−	Continuous inner coating	Single gas	RT, 1−4 bar	13.5	18	[204]

performance" region. For this reason there are only a handful materials that retain their market share for a fairly long time [19]. Composite membranes with new materials in the selective layers were not easy to be commercialized as yet, due to the gap between the lab results and the practical value obtained in industrial conditions.

3.3. CO₂/H₂ separation

Hydrogen is considered the most promising and environment friendly "green" fuel, as the only combustion product is water, which produces no environmental or ecological damage. To date, large-scale hydrogen production generally occurs via steam methane reforming (SMR) followed by the water-gas shift (WGS) reaction, represented by the Eqs. (7) and (8). The final composition of the product from SMR and WGS is largely dependent on the molar steam and carbon ratio, temperature, and pressure.

$$C_nH_m + nH_2O \rightleftharpoons nCO + \left(\frac{m}{2} + n\right)H_2 \tag{7}$$

$$CO + H_2O \rightleftharpoons CO_2 + H_2 \tag{8}$$
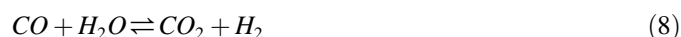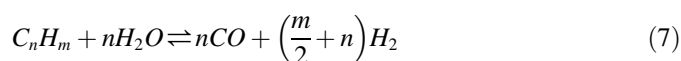
Hydrogen purification is essential to satisfying the various purity requirements for different applications. Since the product leaving the WGS reactor contains primarily H_2 and CO_2, their effective separation is of paramount importance. Hydrogen enrichment can be achieved by various approaches, including pressure swing adsorption (PSA), cryogenic distillation, and membrane separation. The first large application of membranes was hydrogen recovery from ammonia plant purge gas and hydrogen/CO ratio adjustment in syngas/petrochemical plants. Later, the same membranes were also used to recover hydrogen from hydrocarbon and hydro-treater off-gas streams [55].

Although considerable research on polymeric gas-separation membranes has been conducted, specific references that report the gas-transport properties for the H_2/CO_2 gas pair are rather limited. There are two categories of CO_2/H_2 separation membrane: CO_2 selective and H_2 selective membranes. Glassy polymers (e.g. polyimides) are generally used for fabricating H_2-selective membranes with higher thermal stability, while rubbery polymers are commonly used as CO_2-selective membranes. There are different pros and cons for these two category membranes. The first advantage of the H_2-selective membranes is that many H_2-selective membranes can be used at higher operating temperatures compared to CO_2-selective membranes. Moreover, there is no need to remove the impurities in the feed, such as H_2O vapor, CO, HCl, N_2, O_2, BTX (benzene, toluene, xylene), as H_2-selective membranes work predominantly on the principle of diffusivity selectivity; the higher diffusivity of H_2 (compared to the other gases) ensures the exclusion of other gases. However, one serious limitation of using H_2-selective membranes for hydrogen purification is the need to recompress the permeate stream after separation. In addition, high operating pressure may lead to membrane plasticization and reduce the selectivity of H_2 over other gases.

Different from the H_2 selective membranes, CO_2 selective membrane works due to the solubility differences of various gases. The main advantage of the CO_2 selective membrane is that H_2 stays in the retentate, which remains high pressure and thus no recompression is needed for H_2. In addition, the composition of CO_2 in the gas mixture that requires purification is typically much lower than H_2, thus a smaller membrane area is needed compared with the H_2 selective membrane. Third, there is greater scope to increase the reverse gas CO_2/H_2 selectivity by employing facilitated transport membranes since they are not limited by the solution-diffusion mechanism. As always, a coin has two sides: There are disadvantages in CO_2 selective membranes. First, many CO_2 selective membranes prefer a relatively low temperature, as a high temperature will increase the H_2 diffusivity, and hence reduce the CO_2/H_2 selectivity. Second, impurities present in the feed streams with low condensability (e.g. N_2 and O_2), may stay in the retentate with H_2, thus further purification is needed. Some of the up-to-date advances in CO_2/H_2 separation membranes are listed in Table 7.

For CO_2-selective polymeric membranes that do not involve facilitated transport, there seems to be a limitation for the CO_2/H_2 selectivity, which is lower than 15 with only a limited number of exceptions [218]. The relatively weak physical interactions between these polar functional groups and CO_2 molecules may have resulted in the relatively low CO_2/H_2 selectivity. Even more CO_2-philic functional groups could be introduced to render the membranes to be solubility-controlled for CO_2/H_2 separation. For example, Yave et al. introduced tailor-made CO_2-philic additives into a Polyactive polymer matrix by fabricating composite membranes with a selective layer of around 40 nms. High CO_2 permeance was obtained (1777 GPU). However, the CO_2/H_2 selectivity is only around 10 [72]. The operation temperature also has a significant influence on the membrane performances: At a low temperature, the CO_2 solubility increases in the membrane, while the H_2 diffusivity reduces, thus the membrane based on a solution-diffusion mechanism normally shows both higher CO_2 permeability and CO_2/H_2 selectivity at lower temperatures [219].

Ho and co-workers intensively studied a series of amine and salt mobiles carriers (e.g. PAA, PEI, AIBA-K, glycine-Li, 2-aminoisobutyric acid (AIBA-K) and potassium hydroxide (KOH)) in a blend of cross-linked poly(vinyl alcohol) (PVA) and polyallylamine (PAA) [220,221]. Extremely high CO_2 permeability (over 6000 Barrers) and CO_2/H_2 selectivity (over 150) was obtained at high temperatures (over 110 °C) [125]. Later on, the same group investigated the utilization of satirically hindered polyamines as fixed-site carriers, which also resulted in high-performance membranes with a CO_2 permeability of over 6500 Barrer and a CO_2/H_2 selectivity of over 300 at 110 °C [124,156]. The sterically hindered amine is an amine surrounded by a crowded steric environment. The existence of a sterically hindered amine cannot only accelerate the reaction rate between amines and CO_2, but also promote the CO_2 absorption capacities [222−224], resulting in a membrane with both high CO_2 permeability and high CO_2

Table 7
Composite polymeric membranes for CO_2/H_2 separation.

Selective layer Material and thickness (μm)	Supporting materials/surface pore size (nm)	Gutter layer/ thickness (μm)	Fabrication method	Feed gas	Operation conditions	CO_2 permeance (GPU)	CO_2/H_2 selectivity	Ref.
P (DADMACA-co-Vam) (0.5)	PSf (MWCO 6k)	–	Casting	CO_2/H_2 (40/60 by volume)	0.11 Mpa, humid conditions	921	30	[116]
Polyactive (~0.1)	PAN (~20)	PDMS	Dip-coating	Pure gas	293 K, up to 20 bar	2109	7.70	[72]
Polyactive+PEGBE (0.15 −0.5)	PAN (−)	PDMS	Dip-coating	CO_2/H_2 (50/50 by volume)	Feed pressure up to 10 bar and 293 K	888	8−16	[137]
DGBAmE and DAmPEG+TMC (0.8 −1.22)	PSf (MWCO 6k)	PDMS (~0.8)	IP	CO_2/H_2 (40/60 by volume)	0.11 MPa, 100%RH	730	11.0	[144]
DGBAmE+TMC (−)	PSf (MWCO 6k)	PDMS (~0.8)	IP	CO_2/H_2 (15/85 by volume)	0.11 MPa, 100%RH	746	33.9	[145]
PI-ZIF (~4)	Mylar+PI (−)	–	Spin coating	Pure gas	35 °C and 3.5 atm	17.4 Barrers	0.0345	[208]
AIBA-K/polyallylamine/PVA (20−80)	PSf (~50) Teflon (~200)	–	Casting	$CO_2/H_2/N_2$ (20/40/40 by volume)	1.5−2.8 atm, 100−180 °C	8200 Barrers	456	[125]
Dimethylglycine−Li/PVA (30−70)	PSf (−)	–	Casting	$CO_2/H_2/N_2$ (20/40/40 by volume)	90 °C	1700 Barrers	50	[209]
Pebax-RTIL (~0.3)	PAN (~15.7)	PDMS (~1) PTMSP	Dip-coating	CO_2/H_2 (50/50 by volume)	RT	362.1	7.80	[90]
Polaris (−)	–	–	Dip-coating	–	–	1000	45.5	[192]
PVAm+amine (0.2−1.2)	PSf (MWCO 6k)	–	Coating	CO_2/H_2 (40/60 by volume)	0.11 MPa, 100%RH	265	61.6	[210]
PVA+SPBI (15−30)	α-alumina (50−80)	–	Casting	$CO_2/H_2/N_2$ (20/40/40 by volume)	Feed pressure of 220 psia, over 100 °C	1000 Barres	33	[211]
Polyamines+PVA (~25)	PSf (~50)	–	Casting	$CO_2/H_2/N_2$ (20/40/40 by volume)	2 atm, 110 °C	300 Barrers	20−50	[156]
Poly-N-isopropylallylamine in polyvinylalcohol-poly(siloxane) (~25)	PSf (~50)	–	Casting	$CO_2/H_2/N_2$ (20/40/40 by volume)	110 °C and a feed pressure of 2 atm	6500 Barrers	>300	[124]
TMC-amines (~0.2)	PSf (MWCO 6k)	–	IP	CO_2/H_2 mixture (40/60 by volume)	0.11 MPa, 100%RH	350	~10	[212]
Poly(vinyl alcohol) −poly(siloxane)-fumed silica (24−32)	PSf (20)	–	Casting	$CO_2/H_2/N_2$ (20/40/40 by volume)	107 °C and 220 psia	1296 Barrers	87	[213]
Amino salts/Polyamine/PVA (~40)	BHA teflon support	–	Casting	$CO_2/H_2/N_2$ (20/40/40 by volume)	140−150 °C, 0.2 MPa	6000 Barrers	200	[214]
PVA-CNT-amine (10−30)	PSf (~10) PTFE (>30)	–	Casting	$CO_2/H_2/N_2$ (20/40/40 by volume)	107 °C and 15 bar	957 Barrers	17.2	[202]
PVA-amine-CNT (15−30)	PSf (~10)	–	Casting	$CO_2/H_2/N_2$ (20/40/40 by volume)	1.52 MPa and 380.15 K	836 Barrers	43	[215]
PEO-PBT/GO (−)	PAN (−)	–	Dip-coating	–	–	24.9−80.3	10−12	[158]
Cross linked PVA and amine (−)	PSf (~9)	–	Casting	$CO_2/H_2/N_2$ (20/40/40 by volume)	15 bar at 107 °C	920−1300 Barrer	49−88	[216]
Cross linked PVA and amine (10−25)	PSf (~10)	–	Casting	10% CO, 40% H_2 and 50% CO_2	120 °C, 1.1 PSIG	2300−3000	120−180	[217]

selectivity over other gases. It is worth mentioning that, different from general facilitated transport membranes, which suffers from the "carrier saturation" problem at high CO_2 partial pressures, by properly choosing the facilitated transport carriers, such as the PAA and AIBA-K, the facilitated transport membranes achieved a relatively high CO_2/H_2 selectivity larger than 85 and a CO_2 permeability greater than 1000 Barrers at 15 atm and at 106−110 °C [211,213].

Compared with polymeric membranes applying a solution-diffusion mechanism, facilitated transport membranes show both higher CO_2/H_2 selectivity and higher CO_2 permeability. However, developing carriers exhibiting a higher reaction rate and CO_2 absorption capacity along with better long-term stability are desired.

4. Aging, plasticization, long-term stability, and the impacts of impurities

Practically, gas separation membrane should have a lifetime of more than 3−5 years. Membranes that cannot achieve this life-time are unlikely to be used. However, most membranes show a decline of about 30% or even more in gas permeance in 2−3 years, in which most of the decline is in the first six months of operation. Furthermore, real membrane operating conditions may be much harsher than in the lab (e.g. high temperature/pressure, nasty impurities), these conditions may also have negative effects on the long-term performances on the membranes.

4.1. Aging

Glassy polymers are inherently non-equilibrium materials and will go towards the thermodynamic equilibrium state over time. Therefore, their properties are strongly time dependent (e.g., density, refractive index, permeability). The physical aging of bulk polymers has been studied extensively, and several models have been developed to describe the behavior [225]. In early 1990s, researchers found that material behavior is strongly dimension dependent, significant and unpredicted deviations can be found on the same material between a bulk state and thin film state [226,227]. Since then, extensive studies on the influence of physical aging on glassy polymer behavior have been reported in the literature. An excellent summary of physical aging is given in Ref. [228]. Fig. 12 shows the aging behavior of PSf membranes with different thickness. The physical aging was monitored by recording the O_2 and N_2 permeability [229]. Generally, the physical aging rate was found to increase as the film thickness decreases; this means the physical aging can be significant for practical membranes as they normally have a thickness in the micrometer range or even lower. For example, for high free volume polymers (e.g. 6FDA-DAM), an order of magnitude decrease in permeability relative to the initial value over the course of 1000 h of aging was observed in the thin film state, while thick 6FDA-DAM polymer film maintained a relatively high permeability over thousands of hours of aging [230,231]. Therefore, an improved understanding of physical aging rates

will allow more accurate predictions of the long-term performance of composite membranes with a glassy polymer selective layer, which is of crucial importance in designing a membrane system with a satisfactory performance over long service periods.

In the past few years, great efforts have been made to study the thin film physical aging. Many different technologies have been applied to investigating the physical aging of the thin film composite membranes, such as tracking gas permeability [231], ellipsometry [232], fluorescence spectroscopy [233], and energy positron annihilation lifetime spectroscopy technology [234]. Despite the various technologies used to characterize the physical aging for different polymers, their results generally fit well with the gas permeability measurements.

It is commonly accepted that the higher aging rate in thin films compared to bulk polymers is due to the higher diffusion rate of the free volume to the surface. It is also believed that the film has a region of enhanced mobility near the film surfaces, which enhances polymer chain mobility (decreased Tg) and results in accelerated physical aging [235]. Paul et al. intensively investigated the physical aging of different glassy polymers, and mathematic models have been developed [235−241]. Colmenero et al. also thoroughly reviewed the physical aging of glassy polymers and methods to monitor physical aging [242,243]. The dynamics and thermodynamics in physical aging phenomenon were also explained.

The mechanism of the rapid physical aging observed for thin film membranes is not yet fully understood. However, it is clear that several key factors can have a significant effect on the physical aging behavior of the thin films, including:

- Membrane thickness:

Membranes with a thinner thickness present higher physical aging rate, thus new materials/strategies should be developed to have a thin selective layer for composite membranes, while maintaining a low physical aging rate.

- Membrane preparation process/storage history

It is reported that solvents used to prepare a membrane and the membrane's previous processing history have a significant influence on the physical aging [241,244]. In a practical membrane preparation process, these parameters should be taken into consideration.

- Membrane operation temperature/pressure and storage atmosphere

Different temperatures/pressures will influence the diffusion rate of the free volume holes and consequently different physical aging rates. The storage atmosphere also has significant impacts on physical aging.

It is worth emphasizing that in recent decades many different methods have been developed to suppress physical aging, including polymer blending [245], thermal [246]/chemical [247]/UV cross-linking [248], surface plasma
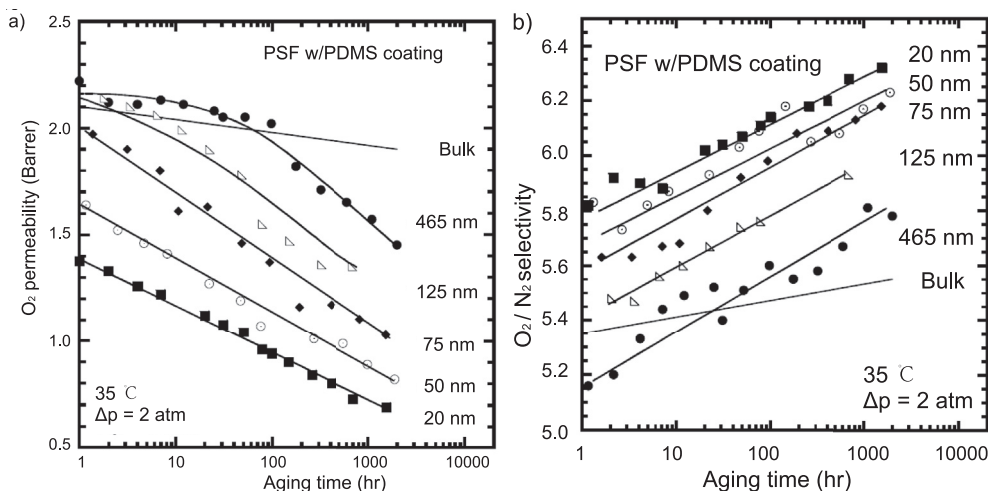
Fig. 12. Influence of physical aging on oxygen permeability (a), and O_2/N_2 pure gas selectivity (b) in PSf films ranging from 465 nm to 20 nm in thickness. Reproduced from Ref. [229].

treatment [249], and the addition of various additives (e.g. nanoparticles) [250−254]. Polymer blending may result in a mixture with better physical aging resistance, but lower permeability and selectivity. Cross-linking is a proven strategy to suppress physical aging, but it normally causes an unavoidable loss in permeability with a gain in selectivity. On the other hand, by properly choosing nano-additives, the incorporation of nanoparticles into the membranes may combine the synergistic properties of enhancing permeability, physical aging resistance, and anti-plasticization characteristics. Thus, incorporating nanoparticles into polymeric membranes can be an effective alternative solution to reduce physical aging.

4.2. Plasticization

It is difficult to give an unambiguous definition of plasticization. Normally, the plasticization of glassy polymers is defined as the increase in gas permeability as a function of feed pressure [255]. The minimum pressure necessary to induce the permeability-increase is called the plasticization pressure. Fig. 13 shows the typical plasticization phenomena of a polymeric membrane. Plasticization needs to be considered specifically for high-pressure CO_2 separation
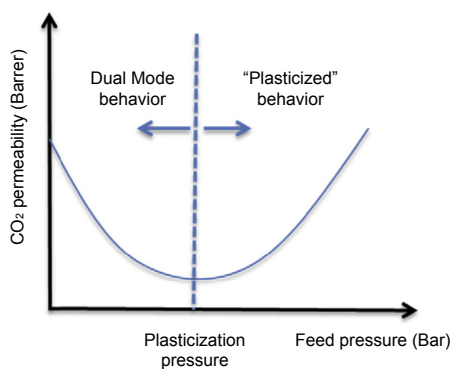

Fig. 13. Typical CO_2 permeation behavior of glassy polymers, reproduced from Ref. [256].

applications. For most of the thick glassy polymeric membranes, CO_2 permeability follows a trend: Decreasing with increasing pressure at low feed pressures, then increasing as the driving pressure is further elevated (as shown in Fig. 13). The first part of the curve can be characterized by the dual sorption behavior, and the second part of the curve can be characterized by the plasticization behavior. This behavior can be explained by the sorption of the highly soluble penetrants (e.g. CO_2 and hydrocarbon vapor), which tend to facilitate the local polymeric segmental rearrangement, thus increasing the free volume and macromolecular chain motion, resulting in an increment of the gas permeability of all gas species but a reduction in the selectivity.

It is well known that the plasticization pressure is thickness dependent [257]. For example, dense 6FDA-DAD at 35 °C is plasticized by 14 bar CO_2 [258], while for asymmetric Matrimid the plasticization pressure is <4 bar [259]. For NG sweetening applications, high pressure CO_2, as well as the heavier hydrocarbon impurities (e.g. C_2H_6, C_3H_8) in the feed stream can cause plasticization and reduce the selectivity of the membrane.

The CO_2 plasticization and conditioning effects in thin glassy polymer films can be different from their behavior in thick membranes. In recent years, researchers have intensively studied the CO_2 plasticization for a series of different glassy polymers, including Matrimid®, polystyrene, polyetherimide, and polysulfone made from bisphenol A (PSF), poly(2,6-dimethyl-1,4-phenylene oxide) (PPO), as well as some amorphous perfluoropolymers [230,235,239,240,260−270]. According to the results, thin films respond more quickly and intensely to plasticizing gases, such as CO_2, than thick films, even at lower pressures. Fig. 14 clearly shows that a Matrimid membrane with a thickness of 20 μms has a much higher plasticization pressure than the same polymer with a thickness of 182 nm. Furthermore, for polymers with different CO_2 solubilities, the degree of plasticization follows the CO_2 solubility in the polymer. In general, for a particular polymer, CO_2 plasticization is a function of film thickness, CO_2
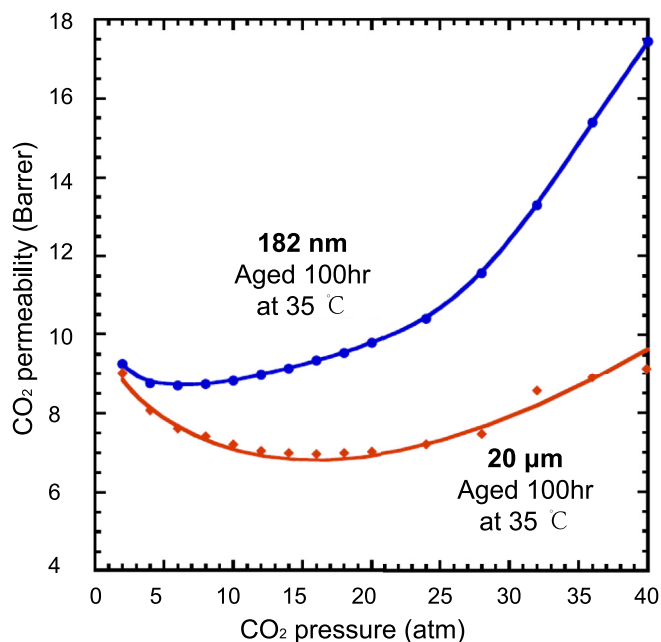
Fig. 14. CO$_2$ plasticization pressure curves for thin and thick Matrimid films with identical prior thermal history. Reproduced from Ref. [240].

pressure, exposure time, aging time, and the prior preparation/storage/thermal treatment history.

A high CO$_2$ pressure will induce both physical aging and plasticization, and these two effects are competing with each other, as can be seen in Fig. 15 [240]. Membranes tested at relatively high operation pressures and temperatures (but lower than the plasticization pressure and Tg) leads to physical aging and decreased gas permeability. Further increasing the CO$_2$ pressure will promote the CO$_2$ molecular penetration through the membrane, and increase the permeability of all gas species. In a short period of time, the CO$_2$ plasticization dominates, and therefore the gas permeability increases. However, after a period of operating, it appears that the tendency for physical aging dominates, and the CO$_2$ permeability goes down over a longer period of time, as shown in Fig. 15. It worth mentioning that in Fig. 15 no reduction can be found for

the membranes with a selective layer of 20 μms in thickness, which is believed mainly because that the CO$_2$ exposure time is not long enough (1000 h).

Various strategies have been applied to reduce the plasticization effect, including cross-linking, thermal annealing, and plasma treatment [263,271–275]. Cross-linking modification has been approved to be an effective approach in suppressing the plasticization phenomenon by different researchers [276–280]. Generally the cross-linking tends to change the chemical structure of the polymers, consequently changing the chains mobility, the interstitial space between chains. Cross-linking will generally result in the reduction of free volume, and a consecutive reduction in gas permeability, but better plasticization resistance. Different methods of cross-linking were summarized in Ref. [276].

Thermal annealing is also widely studied to improve the plasticization resistance of membranes. For example, Chung et al. found that 6FDA-2,6DAT hollow fibers show no increase in CO$_2$ permeance over a wide range of pressures with the membrane being thermal annealed for a period of time over 250 °C [275]. Chen et al. found that thermal annealing at 250 °C for 30 min was sufficient to suppress plasticization for a Matrimid membrane [272]. Different explanations for the effect of thermal annealing have been proposed. Chung et al. stated that the thermal treatment leads to a more compact selective-skin layer and substructure (no cross-linking was observed), which strengthens the anti-plasticization characteristics of the membrane [275]. On the other hand, researchers also proposed that the formation of charge transfer complexes (CTC) during thermal annealing is the main reason for the better anti-plasticization performance [281,282]. Recently, Chen et al. employed the competitive sorption theory to explain the effect of thermal annealing on plasticization. According to their results, the thermal annealing can alternate the ratio of Henry and Langmuir sorption sites and consequently shifts the plasticization pressure to a larger value. The CO$_2$ sorption in Henry's sites is the main contributor to the dilution of the polymer chain and the plasticization, while Langmuir site sorption contributes very little to the plasticization [272].
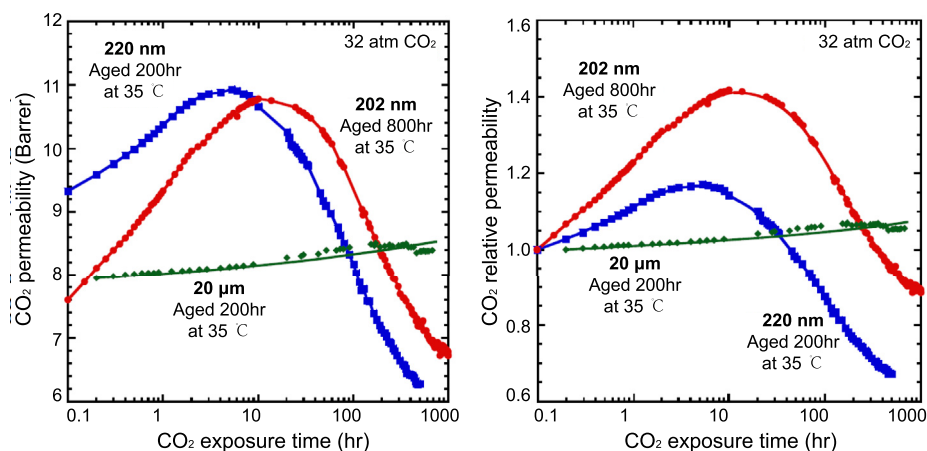

Fig. 15. Physical aging versus CO$_2$ plasticization, reproduced from Ref. [240].

Plasma treatment was also used to improve the anti-plasticization properties of a poly(methyl methacrylate) (PMMA) membrane, as the plasma treatment could lead to surface crosslinking of the PMMA membrane, the resulting membrane exhibited a better plasticization resistance [273].

4.3. Long-term stability and the effects of impurities

Long-term stability is critical for the practical application of membranes. However, it is not realistic to test the long-term stability of the membrane for a period of years in the lab. Many groups carried out their stability tests over few hundreds hour-period, and so far most of the reported membrane separation data are tested in the lab scale using an artificial gas mixture (binary or ternary mixture of CO_2 and other gases). However, in the real gas separation process, there are always different kinds of impurities in the feed stream, for instance, there are SO_x, NO_x, O_2, and fly ashes in the flue gas, while H_2S and heavier hydrocarbons are the main impurities in the raw natural gas or biogas. For many cases, the content of these impurities is relatively small, but they can have significant influences on the separation performances of the membranes. The performance of the membrane reported using idealized simple CO_2/N_2 feed conditions is usually overestimated compared to real industrial conditions. For example, for NG sweetening application, heavier hydrocarbons have a high solubility in the membrane materials; as a consequence, membrane materials will swell and gradually lose selectivity. In post-combustion CO_2 capture, SO_2 can have competitive sorption and reaction with the facilitated transport reagents and reduce the CO_2 permeance. In the past few decades, many researchers have investigated the effect of different impurities for dense membranes with different membrane materials, including an extensive review on this topic [283]. However, reports on the effect of impurities on thin-film composite membranes are limited.

The "conditioning" method is mostly used to investigate the influence of impurities in the feed gas, both for a dense membrane and thin-film composite membranes. Generally, the procedure of this method is to expose the membrane in some simulated gases containing different amounts of impurities for a period of time, from a few days to a few weeks; then the membrane is tested and compared with the fresh membranes without conditioning. Normally a gas mixture with a much higher impurity concentration and higher pressure is used to speed up the influence and shorten the exposure time.

Qiao et al. and Liao et al. investigated the influence of impurities in flue gas on the separation performances using a gas mixture with a much higher impurity concentration to speed up the influence [148,149]. After the membrane was exposed in the gas mixture for a period of time, a clear recovery step of permeance was observed for all the membrane samples, denoting these impurities have a negative effect on the separation performance, but the negative effect of the impurities is reversible. It is found that the presence of impurities leads to a reduction in permeance and CO_2/N_2 selectivity by 28% and 20%, respectively. Li et al. systematically studied the effects of SO_2 concentration on CO_2 separation performances. By increasing SO_2 concentration from 35 to 5000 ppm, the CO_2 permeance and CO_2/N_2 selectivity decrease by 16.6% and 20.2%, indicating that CO_2 separation performance is not sensitive to SO_2 concentration in the feed [131]. In a separate study, the above amine-containing membrane showed stable operation in a 500-h test under simulated flue gas operating conditions with 200 ppm SO_2 and 200 ppm NO_2 [207]. Wang et al. studied the antioxidative properties of their membranes with O2 presence and found a limited influence of O_2 on the separation performances over a period of 400 h [99,284].

Instead of using the conditioning method, Li et al. studied the effects of impurities on their membrane performances using a simulated flue gas, which contains 14.5 vol% CO_2, 6.5 vol% O_2, 100 ppm SO_2, 50 ppm NO_2, 10 ppm CO, balanced by N_2. Performance deterioration is observed when the impurities are present in the feed gas, CO_2 permeance decreased from about 1350 GPU to around 1050 GPU, CO_2/N_2 selectivity decreased from about 125 to 105. However, the membrane performance can gradually recover completely if the impurities are removed from the feed gas, confirming the negative effect of the listed impurities is reversible [116].

For most of the facilitated transport membranes, water vapor is needed to promote the reversible reaction between CO_2 and the reactive group in the membrane matrix. If the humidification is discontinued, generally a sudden decrease in both the CO_2 permeance and CO_2/N_2 selectivity can be observed, as shown in Fig. 16. Fortunately, it is a reversible process: When the feed gas is humidified again, the CO_2 permeance and CO_2/N_2 selectivity can be recovered.

Wang et al. also studied the effects of different coexisting gaseous compounds and fine particles (fly ash) in the flue gas on the PSf asymmetric membranes. According to their results, water vapor can promote the CO_2 separation performances, while the O_2 and SO_2 can slightly inhibit or have a negligible effect on the CO_2 separation performance, respectively. At the same time, the porous fine particles will reduce both CO_2 permeance and CO_2/N_2 selectivity, as it can occupy the effective membrane area and reduce the driving force of CO_2 transport [285].
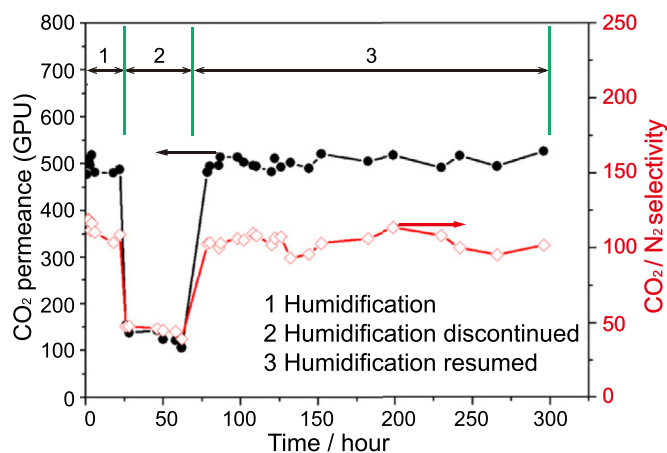

Fig. 16. Influence of water vapor on CO_2 separation performances, reproduced from Ref. [68].

Pilot-scale testing of a polymeric membrane for CO_2 captured in a real flue gas stream from a cement plant was studied by Hägg and co-workers. The membrane was prepared by using a porous polymeric hollow fiber support offered by Air Product with a PVAm coating. Testing was carried out over a 9-month period under real conditions, which contains various impurities such as NO_x, SO_x, and fly ashes. A vacuum was applied on the permeate side to increase the driving force. The membrane showed a relatively stable performance over the whole operation period, demonstrating a good long-term stability of this membrane under industrial condition [179].

The influences of impurities in natural gas sweetening have been intensively studied by Uddin et al. using both conditioning methods and simulated gas containing impurities [196,206,207]. Different impurities such as H_2S, heavier hydrocarbons (e.g. n-hexane and propane), and contaminants from other natural gas treatment processes such as monoethylene glycol and triethylene glycol were investigated. They concluded that the aggressive environment does not introduce permanent damage to the PVAm/PVA blend membrane. These impurities showed a negative effect on the separation performances, but did not destroy the facilitated transport function of the membrane.

All impurity gases (e.g. SO_x, NO_x, heavier hydrocarbons) have negative effects on the separation performances of the membrane, but for some impurities, such as SO_2 and NO_x, the negative effects are reversible, and the membranes can be gradually recovered after the impurities are removed. However, for solid impurities like fly ashes, the negative effects are most likely irreversible as they will occupy the effective membrane surface and reduce the gas permeance permanently. To deal with the impurity problem, the first option is to employ a pre-treatment prior to the membrane module. Apart from that, robust membrane materials that can uphold harsh operational conditions should be used.

5. Conclusions & perspectives

This paper provides a comprehensive review on the advances on multi-layer composite membranes for CO_2 separation in the past 10–15 years. According to the literatures and the discussion, the following conclusions can be drawn:

(1) Facilitated transport material-based composite membranes have been the mostly studied CO_2 separation membranes in recent decades. Many promising results have been obtained, and a few of them have come to a pilot scale.
(2) Glassy-rubbery block copolymers (e.g. Pebax, Polyactive) have been other widely studied selective layer materials for composite membranes. These polymers normally separate CO_2 based on the solution-diffusion mechanism.
(3) Despite the great progress made in developing high-performance glassy polymers (e.g. high free volume polymer), the application of these high free volume glassy polymers in a composite membrane is limited mainly due to the fast physical aging.
(4) Different additives have been used in composite membranes with various purposes, including small molecular

amines, nanoparticles, low molecular weight PEG and ILs. These additives can improve the CO_2 separation performances through different transport mechanisms.
(5) Most of the membrane separation performances reported were tested under a simulated gas mixture without impurities. The performance is probably overestimated. Separation reduction will probably happen with the appearance of impurities in the feed gas.

In summary, membrane material research for gas separation, specifically CO_2 separation, has made great progress in recent decades. However, to make membrane technology more competitive in the industrial market, great efforts are needed. Some perspectives for future research are therefore proposed:

(1) To develop high-performance membrane materials with both high permeability and high selectivity remains the primary and essential part of membrane development.
(2) Economical and environmentally-friendly membrane fabrication process is desired. Despite different membrane configurations and membrane preparation methods reported, less attention has been paid to the membrane fabrication process.
(3) Testing of membranes needs to be done under more realistic and harsher conditions relevant to industrial operation conditions (e.g. SO_x, NO_x, fly ashes etc.). To test the effects of impurities only using conditioning methods with simulated impurities gas may not present a real separation scenario.
(4) Physical aging and plasticization of thin composite membranes need to be further studied with respect to the mechanism and new anti-aging techniques.
(5) Investigating membranes' long-term stabilities under realistic conditions (e.g. various contaminants, high pressures or/and high temperatures etc.), and developing long-lasting membranes.

Conflict of interests

There is no conflict of interest.

Acknowledgements

Abbreviations

6FDA	2,2′-bis(3,4-dicarboxyphenyl) hexafluoropropane dianhydride
CA	Carbonic anhydrase
CNT	Carbon nano tube

CTC	Charge transfer complexes
CVD	Chemical vapor deposition
GPU	Gas permeation unit
MMMs	Mixed matrix membranes
MOF	Metal organic framwork
MWCO	molecular weight cut off
NG	Natural gas
NIPs	Nonsolvent induced phase separation
PAA	Polyallylamine
PAMAM	Polyamidoamine
PAN	Polyacrylonitrile
PANI	Polyaniline
PDMS	polydimethylsiloxane
PEG	Polyethylene glycol
PEI	Polyetherimide
PES	Polyethersulfone
PI	Polyimide
PIL	Poly ionic liquids
PIMs	Polymer of intrinsic microporosity
PMMA	Poly(methyl methacrylate)
PP	Polypropylene
PPO	Poly(p-phenylene oxide)
PSA	Pressure swing adsorption
PSf	Polysulfone
PTFE	Polytetrafluoroethylene
PTMSP	poly(1-(trimethylsilyl)-1-propyne)
PVA	Polyvinyl alcohol
PVAm	Polyvinylamine
PVDF	Polyvinylidene fluoride
PVI	Poly(N-vinylimidazole)
PVP	Polyvinylpyrrolidone
RTIL	Room-temperature ionic liquids
SMR	Steam methane reforming
TFC	Thin film composite
TIPS	Thermally induced phase separation
TMC	Trimesoly Chloride
WGS	Water-gas shift
ZIF	Zeolitic imidazolate framework

References

[1] H.Q. Yang, Z.H. Xu, M.H. Fan, R. Gupta, R.B. Slimane, A.E. Bland, I. Wright, J. Environ. Sci. China 20 (1) (2008) 14−27.

[2] M. Wang, A. Lawal, P. Stephenson, J. Sidders, C. Ramshaw, Chem. Eng. Res. Des. 89 (9) (2011) 1609−1624.

[3] G.T. Rochelle, Science 325 (5948) (2009) 1652−1654.

[4] B.A. Oyenekan, G.T. Rochelle, Ind. Eng. Chem. Res. 45 (8) (2006) 2457−2464.

[5] M.T. Ho, G.W. Allinson, D.E. Wiley, Ind. Eng. Chem. Res. 47 (14) (2008) 4883−4890.

[6] R. Banerjee, A. Phan, B. Wang, C. Knobler, H. Furukawa, M. O'Keeffe, O.M. Yaghi, Science 319 (5865) (2008) 939−943.

[7] C.E. Powell, G.G. Qiao, J. Membr. Sci. 279 (1−2) (2006) 1−49.

[8] E. Favre, Chem. Eng. J. 171 (3) (2011) 782−793.

[9] M.T. Ho, G.W. Allinson, D.E. Wiley, Ind. Eng. Chem. Res. 47 (5) (2008) 1562−1568.

[10] M.B. Hagg, A. Lindbrathen, Ind. Eng. Chem. Res. 44 (20) (2005) 7668−7675.

[11] R. Bredesen, K. Jordal, A. Bolland, Chem. Eng. Process. 43 (9) (2004) 1129−1158.

[12] M.M. Hossain, H.I. de Lasa, Chem. Eng. Sci. 63 (18) (2008) 4433−4451.

[13] A. Lyngfelt, B. Leckner, T. Mattisson, Chem. Eng. Sci. 56 (10) (2001) 3101−3113.

[14] J. Adanez, L.F. de Diego, F. Garcia-Labiano, P. Gayan, A. Abad, J.M. Palacios, Energy Fuels 18 (2) (2004) 371−377.

[15] M.J. Tuinier, M.V. Annaland, G.J. Kramer, J.A.M. Kuipers, Chem. Eng. Sci. 65 (1) (2010) 114−119.

[16] N.H. Duc, F. Chauvy, J.M. Herri, Energy Convers. Manag. 48 (4) (2007) 1313−1322.

[17] H.J. Lee, J.D. Lee, P. Linga, P. Englezos, Y.S. Kim, M.S. Lee, Y.D. Kim, Energy 35 (6) (2010) 2729−2733.

[18] P. Bernardo, E. Drioli, G. Golemme, Ind. Eng. Chem. Res. 48 (10) (2009) 4638−4663.

[19] R.W. Baker, K. Lokhandwala, Ind. Eng. Chem. Res. 47 (7) (2008) 2109−2121.

[20] R.W. Baker, B.T. Low, Macromolecules 47 (20) (2014) 6999−7013.

[21] D.E. Sanders, Z.P. Smith, R.L. Guo, L.M. Robeson, J.E. McGrath, D.R. Paul, B.D. Freeman, Polymer 54 (18) (2013) 4729−4761.

[22] C.H. Lau, P. Li, F.Y. Li, T.S. Chung, D.R. Paul, Prog. Polym. Sci. 38 (5) (2013) 740−766.

[23] M. Rezakazemi, A.E. Amooghin, M.M. Montazer-Rahmati, A.F. Ismail, T. Matsuura, Prog. Polym. Sci. 39 (5) (2014) 817−861.

[24] M.A. Aroon, A.F. Ismail, T. Matsuura, M.M. Montazer-Rahmati, Sep. Purif. Technol. 75 (3) (2010) 229−242.

[25] A.F. Ismail, P.S. Goh, S.M. Sanip, M. Aziz, Sep. Purif. Technol. 70 (1) (2009) 12−26.

[26] T.S. Chung, L.Y. Jiang, Y. Li, S. Kulprathipanja, Prog. Polym. Sci. 32 (4) (2007) 483−507.

[27] H. Li, K. Haas-Santo, U. Schygulla, R. Dittmeyer, Chem. Eng. Sci. 127 (2015) 401−417.

[28] S. Kim, Y.M. Lee, Prog. Polym. Sci. 43 (2015) 1−32.

[29] Z.Y. Yeo, T.L. Chew, P.W. Zhu, A.R. Mohamed, S.P. Chai, J. Porous Mater. 20 (6) (2013) 1457−1475.

[30] N.Y. Du, H.B. Park, M.M. Dal-Cin, M.D. Guiver, Energy Environ. Sci. 5 (6) (2012) 7306−7322.

[31] P.M. Budd, N.B. McKeown, Polym. Chem. 1 (1) (2010) 63−68.

[32] S.L. Qiu, M. Xue, G.S. Zhu, Chem. Soc. Rev. 43 (16) (2014) 6116−6140.

[33] C. Wang, J. Yu, X.J. Hu, Y. Huang, New Carbon Mater. 29 (6) (2014) 409−418.

[34] B.R. Pimentel, A. Parulkar, E.K. Zhou, N.A. Brunelli, R.P. Lively, ChemSusChem 7 (12) (2014) 3202−3240.

[35] H.A. Mannan, H. Mukhtar, T. Murugesan, R. Nasir, D.F. Mohshim, A. Mushtaq, Chem. Eng. Technol. 36 (11) (2013) 1838−1846.

[36] S. Rafiq, L. Deng, M.-B. Hägg, ChemBioEng Rev. 3 (2016) 68−85.

[37] S.L. Liu, L. Shao, M.L. Chua, C.H. Lau, H. Wang, S. Quan, Prog. Polym. Sci. 38 (7) (2013) 1089−1120.

[38] K. Vanherck, G. Koeckelberghs, I.F.J. Vankelecom, Prog. Polym. Sci. 38 (6) (2013) 874−896.

[39] Z. Dai, R.D. Noble, D.L. Gin, X. Zhang, L. Deng, J. Membr. Sci. 497 (2016) 1−20.

[40] Z. Dai, L. Bai, K.N. Hval, X. Zhang, S. Zhang, L. Deng, Sci. China Chem. (2016) 1−9.

[41] Y.W. Jeon, D.H. Lee, Environ. Eng. Sci. 32 (2) (2015) 71−85.

[42] X.Y. Chen, H. Vinh-Thang, A.A. Ramirez, D. Rodrigue, S. Kaliaguine, RSC Adv. 5 (31) (2015) 24399−24448.

[43] E.R. Minardi, S. Chakraborty, V. Calabro, S. Curcio, E. Drioli, RSC Adv. 5 (19) (2015) 14156−14186.

[44] M. Scholz, T. Melin, M. Wessling, Renew. Sustain. Energy Rev. 17 (2013) 199−212.

[45] S. Basu, A.L. Khan, A. Cano-Odena, C.Q. Liu, I.F.J. Vankelecom, Chem. Soc. Rev. 39 (2) (2010) 750−768.

[46] J.K. Adewole, A.L. Ahmad, S. Ismail, C.P. Leo, Int. J. Greenh. Gas Control 17 (2013) 46−65.

[47] Y. Zhang, J. Sunarso, S.M. Liu, R. Wang, Int. J. Greenh. Gas Control 12 (2013) 84−107.

[48] C.A. Scholes, G.W. Stevens, S.E. Kentish, Fuel 96 (1) (2012) 15−28.

[49] Z.Y. Yeo, T.L. Chew, P.W. Zhu, A.R. Mohamed, S.P. Chai, J. Nat. Gas Chem. 21 (3) (2012) 282−298.

[50] P. Luis, T. Van Gerven, B. Van der Bruggen, Prog. Energy Combust. Sci. 38 (3) (2012) 419−448.

[51] C.A. Scholes, K.H. Smith, S.E. Kentish, G.W. Stevens, Int. J. Greenh. Gas Control 4 (5) (2010) 739−755.

[52] K. Ramasubramanian, W.S.W. Ho, Curr. Opin. Chem. Eng. 1 (1) (2011) 47−54.

[53] X. Zhang, B. Singh, X. He, T. Gundersen, L. Deng, S. Zhang, Int. J. Greenh. Gas Control 27 (2014) 289−298.

[54] F. Gallucci, E. Fernandez, P. Corengia, M.V. Annaland, Chem. Eng. Sci. 92 (2013) 40−66.

[55] L. Shao, B.T. Low, T.S. Chung, A.R. Greenberg, J. Membr. Sci. 327 (1−2) (2009) 18−31.

[56] N.W. Ockwig, T.M. Nenoff, Chem. Rev. 107 (10) (2007) 4078−4110.

[57] P. Bakonyi, N. Nemestothy, K. Belafi-Bako, Int. J. Hydrogen Energy 38 (23) (2013) 9673−9687.

[58] R. Faiz, K. Li, Chem. Eng. Sci. 73 (2012) 261−284.

[59] M.T. Ravanchi, T. Kaghazchi, A. Kargari, Desalination 235 (1−3) (2009) 199−244.

[60] L.M. Robeson, J. Membr. Sci. 320 (1−2) (2008) 390−400.

[61] Z.Y. Yeo, S.P. Chai, P.W. Zhu, A.R. Mohamed, RSC Adv. 4 (97) (2014) 54322−54334.

[62] M.H. Wang, V. Janout, S.L. Regen, Acc. Chem. Res. 46 (12) (2013) 2743−2754.

[63] O. Shekhah, J. Liu, R.A. Fischer, C. Woll, Chem. Soc. Rev. 40 (2) (2011) 1081−1106.

[64] S.A. Stern, J. Polym. Sci. Part A 2 Polym. Phys. 6 (11PA) (1968) 1933.

[65] S.H. Yoo, J.H. Kim, J.Y. Jho, J. Won, Y.S. Kang, J. Membr. Sci. 236 (1) (2004) 203−207.

[66] H. Lee, M. Yanilmaz, O. Toprakci, K. Fu, X.W. Zhang, Energy Environ. Sci. 7 (12) (2014) 3857−3886.

[67] P.F. Ji, Y.M. Cao, X.M. Jie, M. Li, Q. Yuan, Sep. Purif. Technol. 71 (2) (2010) 160−167.

[68] S.J. Yuan, Z. Wang, Z.H. Qiao, M.M. Wang, J.X. Wang, S.C. Wang, J. Membr. Sci. 378 (1−2) (2011) 425−437.

[69] T.J. Kim, H. Vralstad, M. Sandru, M.B. Hagg, J. Membr. Sci. 428 (2013) 218−224.

[70] S. Zhao, Z. Wang, Z.H. Qiao, X. Wei, C.X. Zhang, J.X. Wang, S.C. Wang, J. Mater. Chem. A 1 (2) (2013) 246−249.

[71] P.A. Gurr, J.M.P. Scofield, J. Kim, Q. Fu, S.E. Kentish, G.G. Qiao, J. Polym. Sci. Part A Polym. Chem. 52 (23) (2014) 3372−3382.

[72] W. Yave, A. Car, J. Wind, K.V. Peinemann, Nanotechnology 21 (39) (2010).

[73] J.N. Shen, L.G. Wu, D.H. Wang, C.J. Gao, Desalination 223 (1−3) (2008) 425−437.

[74] L. Liu, A. Chakma, X.S. Feng, Ind. Eng. Chem. Res. 44 (17) (2005) 6874−6882.

[75] X.L. Ren, J.Z. Ren, H. Li, S.C. Feng, M.C. Deng, Int. J. Greenh. Gas Control 8 (2012) 111−120.

[76] L.Y. Jiang, T.S. Chung, D.F. Li, C. Cao, A. Kulprathipanja, J. Membr. Sci. 240 (1−2) (2004) 91−103.

[77] E. Lasseuguette, J.C. Rouch, J.C. Remigy, Ind. Eng. Chem. Res. 52 (36) (2013) 13146−13158.

[78] Y. Li, T. Verbiest, I. Vankelecom, J. Membr. Sci. 428 (2013) 63−69.

[79] S. Sridhar, T.M. Aminabhavi, S.J. Mayor, M. Ramakrishna, Ind. Eng. Chem. Res. 46 (24) (2007) 8144−8151.

[80] G.A. Polotskaya, V.P. Sklizkova, N.D. Kozhurnikova, G.K. Elyashevich, V.V. Kudryavtsev, J. Appl. Polym. Sci. 75 (8) (2000) 1026−1032.

[81] M. Sandru, S.H. Haukebo, M.B. Hagg, J. Membr. Sci. 346 (1) (2010) 172−186.

[82] P.T. Nguyen, E. Lasseuguette, Y. Medina-Gonzalez, J.C. Remigy, D. Roizard, E. Favre, J. Membr. Sci. 377 (1−2) (2011) 261−272.

[83] M.Z. Pedram, M. Omidkhah, A.E. Amooghin, J. Ind. Eng. Chem. 20 (1) (2014) 74−82.

[84] J. Huang, J. Zou, W.S.W. Ho, Ind. Eng. Chem. Res. 47 (4) (2008) 1261−1267.

[85] Z. Dai, L. Ansaloni, L. Deng, Ind. Eng. Chem. Res. 55 (20) (2016) 5983−5992.

[86] L.A. El-Azzami, E.A. Grulke, J. Membr. Sci. 323 (2) (2008) 225−234.

[87] L.A. El-Azzami, E.A. Grulke, J. Membr. Sci. 328 (1−2) (2009) 15−22.

[88] T. Masuda, Y. Iguchi, B.Z. Tang, T. Higashimura, Polymer 29 (11) (1988) 2041−2049.

[89] L.M. Robeson, W.F. Burgoyne, M. Langsam, A.C. Savoca, C.F. Tien, Polymer 35 (23) (1994) 4970−4978.

[90] H.Z. Chen, Z.W. Thong, P. Li, T.S. Chung, Int. J. Hydrogen Energy 39 (10) (2014) 5043−5053.

[91] J. Peter, K.V. Peinemann, J. Membr. Sci. 340 (1−2) (2009) 62−72.

[92] S. Harms, K. Ratzke, F. Faupel, N. Chaukura, P.M. Budd, W. Egger, L. Ravelli, J. Adhes. 88 (7) (2012) 608−619.

[93] J.G. Wijmans, R.W. Baker, J. Membr. Sci. 107 (1−2) (1995) 1−21.

[94] R.D. Noble, C.A. Koval, Review of facilitated transport membranes, in: Materials Science of Membranes for Gas and Vapor Separation, John Wiley & Sons, Ltd, 2006, pp. 411−435.

[95] H.C. Ferraz, L.T. Duarte, M. Di Luccio, T.L.M. Alves, A.C. Habert, C.P. Borges, Braz. J. Chem. Eng. 24 (1) (2007) 101−118.

[96] Y.F. Li, S.F. Wang, G.W. He, H. Wu, F.S. Pan, Z.Y. Jiang, Chem. Soc. Rev. 44 (1) (2015) 103−118.

[97] W.J. Ward, W.L. Robb, Science 156 (3781) (1967) 1481.

[98] L.Y. Deng, T.J. Kim, M.B. Hagg, J. Membr. Sci. 340 (1−2) (2009) 154−163.

[99] M.M. Wang, Z. Wang, S.C. Li, C.X. Zhang, J.X. Wang, S.C. Wang, Energy Environ. Sci. 6 (2) (2013) 539−551.

[100] Y.F. Li, Q.P. Xin, H. Wu, R.L. Guo, Z.Z. Tian, Y. Liu, S.F. Wang, G.W. He, F.S. Pan, Z.Y. Jiang, Energy Environ. Sci. 7 (4) (2014) 1489−1499.

[101] M. Saeed, L.Y. Deng, J. Membr. Sci. 494 (2015) 196−204.

[102] K. Yao, Z. Wang, J.X. Wang, S.C. Wang, Chem. Commun. 48 (12) (2012) 1766−1768.

[103] W.R. Browall, Method for sealing breaches in multi-layer ultrathin membrane composites. 1976, Google Patents.

[104] J.M.S. Henis and M.K. Tripodi, Multicomponent membranes for gas separations. 1980, Google Patents.

[105] A. Car, C. Stropnik, W. Yave, K.V. Peinemann, J. Membr. Sci. 307 (1) (2008) 88−95.

[106] M. Maleki, M. Reyssat, F. Restagno, D. Quéré, C. Clanet, J. Colloid Interface Sci. 354 (1) (2011) 359−363.

[107] J. Lee, G. Son, Int. Commun. Heat Mass Transf. 68 (2015) 220−227.

[108] H.C. Mayer, R. Krechetnikov, Phys. Fluids 24 (5) (2012) 052103.

[109] L. Landau, B. Levich, Dragging of a Liquid by a Moving Plate A2 − Pelcé, Pierre, Dynamics of Curved Fronts, Academic Press, San Diego, 1988, pp. 141−153.

[110] M. Guglielmi, S. Zenezini, J. Non Cryst. Solids 121 (1−3) (1990) 303−309.

[111] L. Deng, M.-B. Hägg, Ind. Eng. Chem. Res. 54 (44) (2015) 11139−11150.

[112] J.D. Goddard, J.S. Schultz, S.R. Suchdeo, AIChE J. 20 (4) (1974) 625−645.

[113] J.S. Schultz, J.D. Goddard, S.R. Suchdeo, AIChE J. 20 (3) (1974) 417−445.

[114] R.W. Baker, Membrane Technology and Applications, Wiley, 2003, p. 538.

[115] R.P. Castro, R.W. Baker and J.G. Wijmans, Multilayer interfacial composite membrane. 1991, Google Patents.

[116] P.Y. Li, Z. Wang, Y.N. Liu, S. Zhao, J.X. Wang, S.C. Wang, J. Membr. Sci. 476 (2015) 243−255.

[117] E. Fortunato, P. Barquinha, R. Martins, Adv. Mater. 24 (22) (2012) 2945−2986.

[118] G. Ozaydin-Ince, A.M. Coclite, K.K. Gleason, Rep. Prog. Phys. 75 (1) (2012).

[119] A. Asatekin, K.K. Gleason, Nano Lett. 11 (2) (2011) 677−686.

[120] R. Yang, K.K. Gleason, Langmuir 28 (33) (2012) 12266−12274.

[121] Q.Q. Wang, X.T. Wang, Z.H. Wang, J. Huang, Y. Wang, J. Membr. Sci. 442 (2013) 57−64.

[122] Y. Cai, Z. Wang, C.H. Yi, Y.H. Bai, J.X. Wang, S.C. Wang, J. Membr. Sci. 310 (1−2) (2008) 184−196.

[123] P.Y. Li, Z. Wang, W. Li, Y.N. Liu, J.X. Wang, S.C. Wang, ACS Appl. Mater. Interfaces 7 (28) (2015) 15481−15493.

[124] Y.A. Zhao, W.S.W. Ho, Ind. Eng. Chem. Res. 52 (26) (2013) 8774−8782.

[125] J. Zou, W.S.W. Ho, J. Membr. Sci. 286 (1−2) (2006) 310−321.

[126] M. Acharya, H.C. Foley, J. Membr. Sci. 161 (1−2) (1999) 1−5.

[127] M. Acharya, B.A. Raich, H.C. Foley, M.P. Harold, J.J. Lerou, Ind. Eng. Chem. Res. 36 (8) (1997) 2924−2930.

[128] N. Joseph, P. Ahmadiannamini, R. Hoogenboom, I.F.J. Vankelecom, Polym. Chem. 5 (6) (2014) 1817−1831.

[129] G.J. Zhang, W.L. Gu, S.L. Ji, Z.Z. Liu, Y.L. Peng, Z. Wang, J. Membr. Sci. 280 (1−2) (2006) 727−733.

[130] M.B. Shiflett, H.C. Foley, Science 285 (5435) (1999) 1902−1905.

[131] L.-H. Cheng, Y.-J. Fu, K.-S. Liao, J.-T. Chen, C.-C. Hu, W.-S. Hung, K.-R. Lee, J.-Y. Lai, J. Membr. Sci. 460 (2014) 1−8.

[132] D.Y.C. Leung, G. Caramanna, M.M. Maroto-Valer, Renew. Sustain. Energy Rev. 39 (2014) 426−443.

[133] Y.F. Li, S.F. Wang, H. Wu, R.L. Guo, Y. Liu, Z.Y. Jiang, Z.Z. Tian, P. Zhang, X.Z. Cao, B.Y. Wang, ACS Appl. Mater. Interfaces 6 (9) (2014) 6654−6663.

[134] T.C. Merkel, H.Q. Lin, X.T. Wei, R. Baker, J. Membr. Sci. 359 (1−2) (2010) 126−139.

[135] T.C. Merkel, X.T. Wei, Z.J. He, L.S. White, J.G. Wijmans, R.W. Baker, Ind. Eng. Chem. Res. 52 (3) (2013) 1150−1159.

[136] A. Car, C. Stropnik, W. Yave, K.V. Peinemann, Sep. Purif. Technol. 62 (1) (2008) 110−117.

[137] W. Yave, A. Car, S.S. Funari, S.P. Nunes, K.V. Peinemann, Macromolecules 43 (1) (2010) 326−333.

[138] W. Yave, H. Huth, A. Car, C. Schick, Energy Environ. Sci. 4 (11) (2011) 4656−4661.

[139] J.S. Zhou, M.M. Mok, M.G. Cowan, W.M. McDaniel, T.K. Carlisle, D.L. Gin, R.D. Noble, Ind. Eng. Chem. Res. 53 (51) (2014) 20064−20067.

[140] Q. Fu, A. Halim, J. Kim, J.M.P. Scofield, P.A. Gurr, S.E. Kentish, G.G. Qiao, J. Mater. Chem. A 1 (44) (2013) 13769−13778.

[141] J.M.P. Scofield, P.A. Gurr, J. Kim, Q. Fu, S.E. Kentish, G.G. Qiao, J. Membr. Sci. 499 (2016) 191−200.

[142] S.H. Duan, T. Kouketsu, S. Kazama, K. Yamada, J. Membr. Sci. 283 (1−2) (2006) 2−6.

[143] J. Zhao, Z. Wang, J.X. Wang, S.C. Wang, J. Membr. Sci. 403 (2012) 203−215.

[144] S.C. Li, Z. Wang, C.X. Zhang, M.M. Wang, F. Yuan, J.X. Wang, S.C. Wang, J. Membr. Sci. 436 (2013) 121−131.

[145] S.C. Li, Z. Wang, X.W. Yu, J.X. Wang, S.C. Wang, Adv. Mater. 24 (24) (2012) 3196−3200.

[146] F. Yuan, Z. Wang, S.C. Li, J.X. Wang, S.C. Wang, J. Membr. Sci. 421 (2012) 327−341.

[147] X.W. Yu, Z. Wang, Z.H. Wei, S.J. Yuan, J.A. Zhao, J.X. Wang, S.C. Wang, J. Membr. Sci. 362 (1−2) (2010) 265−278.

[148] Z.H. Qiao, Z. Wang, C.X. Zhang, S.J. Yuan, Y.Q. Zhu, J.X. Wang, S.C. Wang, AIChE J. 59 (1) (2013) 215−228.

[149] J.Y. Liao, Z. Wang, C.Y. Gao, S.C. Li, Z.H. Qiao, M. Wang, S. Zhao, X.M. Xie, J.X. Wang, S.C. Wang, Chem. Sci. 5 (7) (2014) 2843−2849.

[150] S. Zhao, X.C. Cao, Z.J. Ma, Z. Wang, Z.H. Qiao, J.X. Wang, S.C. Wang, Ind. Eng. Chem. Res. 54 (18) (2015) 5139−5148.

[151] L.Y. Deng, M.B. Hagg, J. Membr. Sci. 363 (1−2) (2010) 295−301.

[152] M. Wang, Z. Wang, N. Li, J.Y. Liao, S. Zhao, J.X. Wang, S.C. Wang, J. Membr. Sci. 495 (2015) 252−268.

[153] J.H. Oh, Y.S. Kang, S.W. Kang, Chem. Commun. 49 (86) (2013) 10181−10183.

[154] I.S. Chae, M. Kim, Y.S. Kang, S.W. Kang, J. Membr. Sci. 466 (2014) 357−360.

[155] C.H. Park, J.H. Lee, J.P. Jung, B. Jung, J.H. Kim, J. Membr. Sci. 492 (2015) 452−460.

[156] Y.N. Zhao, W.S.W. Ho, J. Membr. Sci. 415 (2012) 132−138.

[157] Y. Chen, L. Zhao, B. Wang, P. Dutta, W.S. Winston Ho, J. Membr. Sci. 497 (2016) 21−28.

[158] M. Karunakaran, R. Shevate, M. Kumar, K.V. Peinemann, Chem. Commun. 51 (75) (2015) 14187−14190.

[159] A. Mondal, B. Mandal, J. Membr. Sci. 460 (2014) 126−138.

[160] A. Halim, Q. Fu, Q. Yong, P.A. Gurr, S.E. Kentish, G.G. Qiao, J. Mater. Chem. A 2 (14) (2014) 4999−5009.

[161] Q. Fu, E.H.H. Wong, J. Kim, J.M.P. Scofield, P.A. Gurr, S.E. Kentish, G.G. Qiao, J. Mater. Chem. A 2 (42) (2014) 17751−17756.

[162] S. Tan, Q. Fu, J.M.P. Scofield, J. Kim, P.A. Gurr, K. Ladewig, A. Blencowe, G.G. Qiao, J. Mater. Chem. A 3 (28) (2015) 14876−14886.

[163] Q. Fu, J. Kim, P.A. Gurr, J.M.P. Scofield, S.E. Kentish, G.G. Qiao, Energy Environ. Sci. 9 (2016) 434−440.

[164] J.M.P. Scofield, P.A. Gurr, J. Kim, Q. Fu, A. Halim, S.E. Kentish, G.G. Qiao, J. Polym. Sci. Part A Polym. Chem. 53 (12) (2015) 1500−1511.

[165] Y. Dai, X. Ruan, F. Bai, M. Yu, H. Li, Z. Zhao, G. He, Appl. Surf. Sci. 360 (Part A) (2016) 164−173.

[166] F. Nie, G.H. He, W. Zhao, J. Ju, Y.F. Liu, Y. Dai, J. Polym. Res. 21 (1) (2013).

[167] P. Li, H.Z. Chen, T.-S. Chung, J. Membr. Sci. 434 (2013) 18−25.

[168] Y.Y. Wang, T. Hu, H.Y. Li, G.X. Dong, W. Wong and V. Chen, Enhancing membrane permeability for CO₂ capture through blending commodity polymers with selected PEO and PEO-PDMS copolymers and composite hollow fibres. 12th International Conference on Greenhouse Gas Control Technologies, Ghgt-12, 2014. vol. 63: pp. 202−209.

[169] L. Liu, A. Chakma, X. Feng, Chem. Eng. J. 105 (1−2) (2004) 43−51.

[170] A.K. Zulhairun, Z.G. Fachrurrazi, M.N. Izwanne, A.F. Ismail, Sep. Purif. Technol. 146 (2015) 85−93.

[171] Y. Choi, Y.R. Kim, Y.S. Kang, S.W. Kang, Chem. Eng. J. 279 (2015) 273−276.

[172] T. Koschine, K. Ratzke, F. Faupel, M.M. Khan, T. Emmler, V. Filiz, V. Abetz, L. Ravelli, W. Egger, J. Polym. Sci. Part B Polym. Phys. 53 (3) (2015) 213−217.

[173] L. Deng, M.-B. Hägg, Int. J. Greenh. Gas Control 26 (0) (2014) 127−134.

[174] M. Wang, Z. Wang, N. Li, J. Liao, S. Zhao, J. Wang, S. Wang, J. Membrane Sci. 495 (2015) 252−268.

[175] J.E. Bara, D.E. Camper, D.L. Gin, R.D. Noble, Acc. Chem. Res. 43 (1) (2009) 152−159.

[176] J. Deng, L. Bai, S. Zeng, X.-P. Zhang, Y. Nie, L. Deng, S. Zhang, RSC Adv. 6 (2016) 45184−45192.

[177] K. Ramasubramanian, Y.N. Zhao, W.S.W. Ho, AIChE J. 59 (4) (2013) 1033−1045.

[178] L. Deng, T.J. Kim, M.B. Hagg, Desalination 199 (1−3) (2006) 523−524.

[179] Xuezhong He, May-Britt Hägg, Vahid Sarfarez, Marius Sandru, T.-J. Kim, Demonstration on CO₂ capture using a membrane pilot process at cement factory in Brevik Norway − lessons learnt, in: Euromembrane 2015, 2015. Aachen, Germany.

[180] Y.F. Li, Q.P. Xin, S.F. Wang, Z.Z. Tian, H. Wu, Y. Liu, Z.Y. Jiang, Chem. Commun. 51 (10) (2015) 1901−1904.

[181] Y.F. Li, X.Q. Li, H. Wu, Q.P. Xin, S.F. Wang, Y. Liu, Z.Z. Tian, T.T. Zhou, Z.Y. Jiang, H.W. Tian, X.Z. Cao, B.Y. Wang, J. Membr. Sci. 493 (2015) 460−469.

[182] S. Kumar, J.H. Cho, I. Moon, Int. J. Greenh. Gas Control 20 (2014) 87−116.

[183] J. Haggin, Chem. Eng. News 66 (23) (1988) 7−16.

[184] L.Y. Jiang, Y. Wang, T.S. Chung, X.Y. Qiao, J.Y. Lai, Prog. Polym. Sci. 34 (11) (2009) 1135−1160.

[185] Y.C. Xiao, B.T. Low, S.S. Hosseini, T.S. Chung, D.R. Paul, Prog. Polym. Sci. 34 (6) (2009) 561−580.

[186] N.B. McKeown, P.M. Budd, Macromolecules 43 (12) (2010) 5163−5176.

[187] D. Bastani, N. Esmaeili, M. Asadollahi, J. Ind. Eng. Chem. 19 (2) (2013) 375−393.

[188] H.B.T. Jeazet, C. Staudt, C. Janiak, Dalton Trans. 41 (46) (2012) 14003−14027.

[189] G.X. Dong, H.Y. Li, V.K. Chen, J. Mater. Chem. A 1 (15) (2013) 4610−4630.

[190] S. Sridhar, B. Smitha, T.M. Aminabhavi, Sep. Purif. Rev. 36 (2) (2007) 113−174.

[191] N.V. Blinova, F. Svec, J. Membr. Sci. 423 (2012) 514−521.

[192] H. Lin, Z. He, Z. Sun, J. Vu, A. Ng, M. Mohammed, J. Kniep, T.C. Merkel, T. Wu, R.C. Lambrecht, J. Membr. Sci. 457 (2014) 149−161.

[193] Z. Wang, M. Li, Y. Cai, J.X. Wang, S.C. Wang, J. Membr. Sci. 290 (1−2) (2007) 250−258.

[194] Y. Zhang, Z. Wang, S.C. Wang, Desalination 145 (1−3) (2002) 385−388.

[195] C.H. Yi, Z. Wang, M. Li, J.X. Wang, S.C. Wang, Desalination 193 (1−3) (2006) 90−96.

[196] M.W. Uddin, M.B. Hagg, J. Membr. Sci. 423 (2012) 143−149.

[197] L.Y. Deng, M.B. Hagg, Int. J. Greenh. Gas Control 4 (4) (2010) 638−646.

[198] T.J. Kim, B.A. Li, M.B. Hagg, J. Polym. Sci. Part B Polym. Phys. 42 (23) (2004) 4326−4336.

[199] X.Z. He, T.J. Kim, M.B. Hagg, J. Membr. Sci. 470 (2014) 266−274.

[200] X.Z. He, M.B. Hagg, T.J. Kim, AIChE J. 60 (12) (2014) 4174−4184.

[201] J.J. Qin, T.S. Chung, Desalination 192 (1−3) (2006) 112−116.

[202] L. Ansaloni, Y.N. Zhao, B.T. Jung, K. Ramasubramanian, M.G. Baschetti, W.S.W. Ho, J. Membr. Sci. 490 (2015) 18−28.

[203] J. Zhao, Z. Wang, J.X. Wang, S.C. Wang, J. Membr. Sci. 283 (1−2) (2006) 346−356.

[204] E. Esposito, G. Clarizia, P. Bernardo, J.C. Jansen, Z. Sedláková, P. Izák, S. Curcio, B. de Cindio, F. Tasselli, Chem. Eng. Process. Process Intensif. 94 (2015) 53−61.

[205] P. Luangrujiwong, A. Sungpet, R. Jiraratananon, J.D. Way, J. Membr. Sci. 250 (1−2) (2005) 277−282.

[206] M.W. Uddin, M.B. Hagg, J. Membr. Sci. 423 (2012) 150−158.

[207] T.J. Kim, M.W. Uddin, M. Sandru, M.B. Hagg, The effect of contaminants on the composite membranes for CO_2 separation and challenges in up-scaling of the membranes, in: 10th International Conference on Greenhouse Gas Control Technologies, vol. 4, 2011, pp. 737−744.

[208] S.N. Wijenayake, N.P. Panapitiya, C.N. Nguyen, Y. Huang, K.J. Balkus, I.H. Musselman, J.P. Ferraris, Sep. Purif. Technol. 135 (2014) 190−198.

[209] Y.H. Tee, J. Zou, W.S.W. Ho, J. Chin. Inst. Chem. Eng. 37 (1) (2006) 37−47.

[210] Z.H. Qiao, Z. Wang, S.J. Yuan, J.X. Wang, S.C. Wang, J. Membr. Sci. 475 (2015) 290−302.

[211] H. Bai, W.S.W. Ho, Ind. Eng. Chem. Res. 50 (21) (2011) 12152−12161.

[212] W.J. He, Z. Wang, W. Li, S.C. Li, Z.H. Bai, J.X. Wang, S.C. Wang, J. Membr. Sci. 476 (2015) 171−181.

[213] R. Xing, W.S.W. Ho, J. Membr. Sci. 367 (1−2) (2011) 91−102.

[214] J. Zou, W.S.W. Ho, J. Chem. Eng. Jpn. 40 (11) (2007) 1011−1020.

[215] Y.A. Zhao, B.T. Jung, L. Ansaloni, W.S.W. Ho, J. Membr. Sci. 459 (2014) 233−243.

[216] V. Vakharia, K. Ramasubramanian, W.S.W. Ho, J. Membr. Sci. 488 (2015) 56−66.

[217] Z. Tong, V.K. Vakharia, M. Gasda, W.S.W. Ho, React. Funct. Polym. 86 (2015) 111−116.

[218] P. Li, Z. Wang, Z. Qiao, Y. Liu, X. Cao, W. Li, J. Wang, S. Wang, J. Membr. Sci. 495 (2015) 130−168.

[219] H.Q. Lin, E. Van Wagner, B.D. Freeman, L.G. Toy, R.P. Gupta, Science 311 (5761) (2006) 639−642.

[220] W.S.W. Ho, Membranes comprising salts of aminoacids in hydrophilic polymers. 1997, Google Patents.

[221] W.S.W. Ho, Membranes comprising aminoacid salts in polyamine polymers and blends. 2000, Google Patents.

[222] M.J. Horvath, D. Saylik, P.S. Elmes, W.R. Jackson, C.G. Lovel, K. Moody, Tetrahedron Lett. 40 (2) (1999) 363−366.

[223] T. Mimura, T. Suda, I. Iwaki, A. Honda, H. Kumazawa, Chem. Eng. Commun. 170 (1998) 245−260.

[224] G. Sartori, D.W. Savage, Ind. Eng. Chem. Fundam. 22 (2) (1983) 239−249.

[225] A.J. Kovacs, J.J. Aklonis, J.M. Hutchinson, A.R. Ramos, J. Polym. Sci. Part B Polym. Phys. 17 (7) (1979) 1097−1162.

[226] M.E. Rezac, P.H. Pfromm, L.M. Costello, W.J. Koros, Ind. Eng. Chem. Res. 32 (9) (1993) 1921−1926.

[227] P.H. Pfromm, W.J. Koros, Polymer 36 (12) (1995) 2379−2387.

[228] B.W. Rowe, B.D. Freeman, D.R. Paul, Chapter 3 physical aging of membranes for gas separations, in: Membrane Engineering for the Treatment of Gases: Volume 1: Gas-separation Problems with MembranesThe Royal Society of Chemistry, 2011, pp. 58−83.

[229] B.W. Rowe, B.D. Freeman, D.R. Paul, Polymer 50 (23) (2009) 5565−5575.

[230] L.L. Cui, W.L. Qiu, D.R. Paul, W.J. Koros, Polymer 52 (24) (2011) 5528−5537.

[231] L.L. Cui, W.L. Qiu, D.R. Paul, W.J. Koros, Polymer 52 (15) (2011) 3374−3380.

[232] E.A. Baker, P. Rittigstein, J.M. Torkelson, C.B. Roth, J. Polym. Sci. Part B Polym. Phys. 47 (24) (2009) 2509−2519.

[233] C.J. Ellison, S.D. Kim, D.B. Hall, J.M. Torkelson, Eur. Phys. J. E 8 (2) (2002) 155−166.

[234] B.W. Rowe, S.J. Pas, A.J. Hill, R. Suzuki, B.D. Freeman, D.R. Paul, Polymer 50 (25) (2009) 6149−6156.

[235] T.M. Murphy, S.D. Freeman, D.R. Paul, Polymer 54 (2) (2013) 873−880.

[236] Y. Huang, X. Wang, D.R. Paul, J. Membr. Sci. 277 (1−2) (2006) 219−229.

[237] Y. Huang, D.R. Paul, Macromolecules 38 (24) (2005) 10148−10154.

[238] J.H. Kim, W.J. Koros, D.R. Paul, Polymer 47 (9) (2006) 3104−3111.

[239] J.Z. Xia, T.S. Chung, P. Li, N.R. Horn, D.R. Paul, Polymer 53 (10) (2012) 2099−2108.

[240] N.R. Horn, D.R. Paul, Polymer 52 (7) (2011) 1619−1627.

[241] B.W. Rowe, B.D. Freeman, D.R. Paul, Polymer 51 (16) (2010) 3784−3792.

[242] D. Cangialosi, V.M. Boucher, A. Alegria, J. Colmenero, Soft Matter 9 (36) (2013) 8619−8630.

[243] D. Cangialosi, A. Alegría and J. Colmenero, Prog. Polym. Sci.

[244] R.R. Tiwari, Z.P. Smith, H.Q. Lin, B.D. Freeman, D.R. Paul, Polymer 55 (22) (2014) 5788−5800.

[245] K. Nagai, S. Kanehashi, S. Tabei, T. Nakagawa, J. Membr. Sci. 251 (1−2) (2005) 101−110.

[246] F.Y. Li, Y.C. Xiao, T.S. Chung, S. Kawi, Macromolecules 45 (3) (2012) 1427−1437.

[247] S.D. Kelman, B.W. Rowe, C.W. Bielawski, S.J. Pas, A.J. Hill, D.R. Paul, B.D. Freeman, J. Membr. Sci. 320 (1−2) (2008) 123−134.

[248] M.S. McCaig, D.R. Paul, Polymer 40 (26) (1999) 7209−7225.

[249] L. Shao, J. Samseth, M.B. Hagg, Plasma Process. Polym. 4 (9) (2007) 823−831.

[250] D. Gomes, S.P. Nunes, K.V. Peinemann, J. Membr. Sci. 246 (1) (2005) 13−25.

[251] E.R. Rangel, E.M. Maya, F. Sanchez, J. de Abajo, J.G. de la Campa, J. Membr. Sci. 447 (2013) 403−412.

[252] S. Matteucci, V.A. Kusuma, S.D. Kelman, B.D. Freeman, Polymer 49 (6) (2008) 1659−1675.

[253] C.H. Lau, P.T. Nguyen, M.R. Hill, A.W. Thornton, K. Konstas, C.M. Doherty, R.J. Mulder, L. Bourgeois, A.C.Y. Liu, D.J. Sprouster, J.P. Sullivan, T.J. Bastow, A.J. Hill, D.L. Gin, R.D. Noble, Angew. Chem. Int. Ed. 53 (21) (2014) 5322−5326.

[254] C.H. Lau, K. Konstas, A.W. Thornton, A.C.Y. Liu, S. Mudie, D.F. Kennedy, S.C. Howard, A.J. Hill, M.R. Hill, Angew. Chem. Int. Ed. 54 (9) (2015) 2669−2673.

[255] A. Bos, I.G.M. Punt, M. Wessling, H. Strathmann, J. Membr. Sci. 155 (1) (1999) 67−78.

[256] A.F. Ismail, W. Lorna, Sep. Purif. Technol. 27 (3) (2002) 173−194.

[257] S.M. Jordan, M.A. Henson, W.J. Koros, J. Membr. Sci. 54 (1−2) (1990) 103−118.

[258] X. Duthie, S. Kentish, C. Powell, K. Nagai, G. Qiao, G. Stevens, J. Membr. Sci. 294 (1−2) (2007) 40−49.

[259] G.C. Kapantaidakis, G.H. Koops, M. Wessling, S.P. Kaldis, G.P. Sakellaropoulos, AIChE J. 49 (7) (2003) 1702—1711.
[260] N.R. Horn, D.R. Paul, Macromolecules 45 (6) (2012) 2820—2834.
[261] R.R. Tiwari, Z.P. Smith, H.Q. Lin, B.D. Freeman, D.R. Paul, Polymer 61 (2015) 1—14.
[262] J.Z. Xia, T.S. Chung, D.R. Paul, J. Membr. Sci. 450 (2014) 457—468.
[263] J.X. Zhou, A.T. Haldeman, E.H. Wagener, S.M. Husson, J. Membr. Sci. 454 (2014) 398—406.
[264] H. Wang, T.S. Chung, D.R. Paul, J. Membr. Sci. 458 (2014) 27—35.
[265] M. Wessling, M.L. Lopez, H. Strathmann, Sep. Purif. Technol. 24 (1—2) (2001) 223—233.
[266] T. Visser, N. Masetto, M. Wessling, J. Membr. Sci. 306 (1—2) (2007) 16—28.
[267] T. Visser, G.H. Koops, M. Wessling, J. Membr. Sci. 252 (1—2) (2005) 265—277.
[268] C.A. Scholes, G.Q. Chen, G.W. Stevens, S.E. Kentish, J. Membr. Sci. 346 (1) (2010) 208—214.
[269] N.R. Horn, D.R. Paul, Polymer 52 (24) (2011) 5587—5594.
[270] K. Simons, K. Nijmeijer, J.E. Bara, R.D. Noble, M. Wessling, J. Membr. Sci. 360 (1—2) (2010) 202—209.
[271] C. Zhou, T.S. Chung, R. Wang, Y. Liu, S.H. Goh, J. Membr. Sci. 225 (1—2) (2003) 125—134.
[272] G.X. Dong, H.Y. Li, V. Chen, J. Membr. Sci. 369 (1—2) (2011) 206—220.
[273] C.C. Hu, C.Y. Tu, Y.C. Wang, C.L. Li, K.R. Lee, J.Y. Lai, J. Appl. Polym. Sci. 93 (1) (2004) 395—401.
[274] C.C. Chen, S.J. Miller, W.J. Koros, Ind. Eng. Chem. Res. 52 (3) (2013) 1015—1022.
[275] T.S. Chung, J.H. Ren, R. Wang, D.F. Li, Y. Liu, K.P. Pramoda, C. Cao, W.W. Loh, J. Membr. Sci. 214 (1) (2003) 57—69.
[276] J.D. Wind, C. Staudt-Bickel, D.R. Paul, W.J. Koros, Ind. Eng. Chem. Res. 41 (24) (2002) 6139—6148.
[277] W.L. Qiu, C.C. Chen, L.R. Xu, L.L. Cui, D.R. Paul, W.J. Koros, Macromolecules 44 (15) (2011) 6046—6056.
[278] A.M. Kratochvil, W.J. Koros, Macromolecules 41 (21) (2008) 7920—7927.
[279] A.M.W. Hillock, W.J. Koros, Macromolecules 40 (3) (2007) 583—587.
[280] L. Shao, T.S. Chung, S.H. Goh, K.P. Pramoda, J. Membr. Sci. 256 (1—2) (2005) 46—56.
[281] F.B. Zhou, W.J. Koros, Polymer 47 (1) (2006) 280—288.
[282] J.J. Krol, M. Boerrigter, G.H. Koops, J. Membr. Sci. 184 (2) (2001) 275—286.
[283] C. Scholes, S. Kentish, G. Stevens, Sep. Purif. Rev. 38 (1) (2009) 1—44.
[284] M.M. Wang, Z. Wang, J.X. Wang, Y.Q. Zhu, S.C. Wang, Energy Environ. Sci. 4 (10) (2011) 3955—3959.
[285] X. Wang, H. Chen, L. Zhang, R. Yu, R.M. Qu, L.J. Yang, J. Membr. Sci. 470 (2014) 237—245.